

STUDY ON THE RESPONSES OF GLUTATHIONE S-  
TRANSFERASE *Acidovorax* sp. KKS102 TOWARDS  
ANTIBIOTICS

ROSALIA RANI

FACULTY OF SCIENCE  
UNIVERSITI MALAYA  
KUALA LUMPUR

2022

**STUDY ON THE RESPONSES OF GLUTATHIONE S-  
TRANSFERASE *Acidovorax* sp. KKS102 TOWARDS  
ANTIBIOTICS**

**ROSALIA RANI**

**DISSERTATION SUBMITTED IN FULFILMENT OF  
THE REQUIREMENTS FOR THE DEGREE OF MASTER  
OF SCIENCE**

**INSITUTE OF BIOLOGICAL SCIENCE  
FACULTY OF SCIENCE  
UNIVERSITI MALAYA  
KUALA LUMPUR**

**2022**

UNIVERSITI MALAYA

**ORIGINAL LITERARY WORK DECLARATION**

Name of Candidate: **ROSALIA RANI**

Registration/Matric No: **17198124/1 SMA180035**

Name of Degree: **MASTER OF SCIENCE**

Title of Dissertation ("this Work"):

**STUDY ON THE RESPONSES OF GLUTATHIONE S-TRANSFERASE OF  
*Acidovorax* sp. KKS102 TOWARDS ANTIBIOTICS**

Field of Study: **BIOCHEMISTRY**

I do solemnly and sincerely declare that:

- (1) I am the sole author/writer of this Work;
- (2) This Work is original;
- (3) Any use of any work in which copyright exists was done by way of fair dealing and for permitted purposes and any excerpt or extract from, or reference to or reproduction of any copyright work has been disclosed expressly and sufficiently and the title of the Work and its authorship have been acknowledged in this Work;
- (4) I do not have any actual knowledge nor do I ought reasonably to know that the making of this work constitutes an infringement of any copyright work;
- (5) I hereby assign all and every rights in the copyright to this Work to the University of Malaya ("UM"), who henceforth shall be owner of the copyright in this Work and that any reproduction or use in any form or by any means whatsoever is prohibited without the written consent of UM having been first had and obtained;
- (6) I am fully aware that if in the course of making this Work I have infringed any copyright whether intentionally or otherwise, I may be subject to legal action or any other action as may be determined by UM.

Candidate's Signature:

Date: 23 May 2022

Subscribed and solemnly declared before,

Witness's Signature:

Date: 23 May 2022

Name:

Designation:

# STUDY ON THE RESPONSES OF GLUTATHIONE S-TRANSFERASE *Acidovorax* sp. KKS102 TOWARDS ANTIBIOTICS

## ABSTRACT

Beta class glutathione S-transferase (GST) activity is known to be associated with antibiotic resistance, one of the most serious threats to global health. In this research, the study of antibiotic resistance developed by beta class GST was conducted using KKSG6, one of the GST isozymes found in *Acidovorax* sp. KKS102. The KKSG6 gene has been successfully expressed in *Escherichia coli* BL21 Star™ (DE3) using pET101/D-TOPO®-KKSG6 as an expression vector, resulting in the presence of a protein band around 20 kDa. KKSG6 protein has also been successfully purified using GSTrap™ HP column. Optimisation expression showed that KKSG6 exhibits its optimum activity when the culture was incubated 5 hours after the addition of 0.1 mM IPTG. Over-expression of KKSG6 made *Escherichia coli* BL21 Star™ (DE3) to be less susceptible towards kanamycin, streptomycin, gentamycin, tetracycline and chloramphenicol, suggesting the antibiotics binding with KKSG6. Our study has shown that chloramphenicol inhibited the conjugation activity of the enzyme towards CDNB. An *in-silico* study using protein-ligand docking predicted that antibiotics binding could take place at the protein dimer interface and H-site depending on their properties.

**Keywords:** Glutathione S-transferase, beta class, antibiotic resistance, molecular docking.

# KAJIAN KE ATAS TINDAK BALAS GLUTATHIONE S-TRANSFERASE *Acidovorax* sp. KKS102 TERHADAP ANTIBIOTIK

## ABSTRAK

Aktiviti glutathione S-transferase (GST) kelas beta diketahui berkaitan dengan ketahanan terhadap antibiotik, yang merupakan salah satu ancaman paling serius dalam dunia kesihatan. Dalam penyelidikan ini, kajian ketahanan terhadap antibiotik yang disebabkan oleh GST kelas beta dilakukan menggunakan KKSG6, salah satu isoenzim GST yang terdapat dalam *Acidovorax* sp. KKS102. Gen KKSG6 telah berjaya diekspresi dalam *Escherichia coli* BL21 Star™ (DE3) dengan menggunakan pET101/D-TOPO®-KKSG6 sebagai vektor ekspresi, yang mengakibatkan adanya jalur protein dengan ukuran sekitar 20 kDa. Protein KKSG6 juga telah berhasil dimurnikan menggunakan lajur GSTrap™ HP. Optimasi ekspresi menunjukkan bahwa KKSG6 mencapai aktiviti optimumnya ketika kultur diinkubasi selama 5 jam setelah penambahan 0.1 mM IPTG. Over-ekspresi KKSG6 menyebabkan *Escherichia coli* BL21 Star™ (DE3) menjadi kurang rentan terhadap kanamisin, streptomisin, gentamisin, tetrasiklin dan kloramfenikol, yang menunjukkan adanya pengikatan antibiotik dengan KKSG6. Kajian kami menunjukkan bahawa kloramfenikol menghalang aktiviti konjugasi enzim ke CDNB. Kajian *in-silico* menggunakan doking protein-ligan meramalkan bahawa pengikatan antibiotic yang berlaku di antara muka dimer protein dan tapak H adalah bergantung pada ciri-cirinya.

**Kata kunci:** Glutathione S-transferase, kelas beta, ketahanan antibiotik, dok molekular.

## ACKNOWLEDGEMENTS

Alhamdu lillaahi robbil ‘aalamiin. I praise and thank Allah, the only God, for giving me health, strenght and ease to complete my dissertation.

I would also like to thank my supervisors, Associate Professor Dr. Zazali bin Alias and Dr. Khanom binti Simarani for their guidance and motivations for the last two years. May Allah grant you both health so that you can continue assisting other students in pursuing their dreams.

My wholehearted thanks go to my friends, who are always there for me when I am down. Thank you for being a good listener. Wherever you are, whatever you do, may Allah protect you from bad things, ease your plans and help you through the hardships.

Finally and the most importantly, I want to express my special gratitude to my parents, ayah and bunda, my support system, who constantly pray for my success. May Allah bless you with rizq, health and happiness. I hope that one day I can make both of you proud.

## TABLE OF CONTENTS

<b>ABSTRACT</b>	<b>iii</b>
<b>ABSTRAK</b>	<b>iv</b>
<b>ACKNOWLEDGEMENTS</b>	<b>v</b>
<b>TABLE OF CONTENTS</b>	<b>vi</b>
<b>LIST OF FIGURES</b>	<b>xi</b>
<b>LIST OF TABLES</b>	<b>xiii</b>
<b>LIST OF SYMBOLS AND ABBREVIATIONS</b>	<b>xiv</b>
<b>LIST OF APPENDICES</b>	<b>xv</b>
<b>CHAPTER 1: INTRODUCTION</b>	<b>16</b>
1.1 General introduction	16
1.2 Problem statement	17
1.3 Objectives	17
<b>CHAPTER 2: LITERATURE REVIEW</b>	<b>18</b>
2.1 Antibiotics	18
2.1.1 Mechanisms	19
2.1.1.1 Cell wall synthesis inhibition	19
2.1.1.2 Protein synthesis inhibition	19
2.1.1.3 DNA synthesis inhibition	20
2.1.1.4 RNA synthesis inhibition	20
2.1.1.5 Folic acid synthesis inhibition	21
2.1.2 Classification	22
2.2 Antibiotic resistance	23
2.2.1 Current status	23
2.2.2 Mechanisms and origin	24
2.3 Glutathione S-transferase	25
2.3.1 Functions of GST	26
2.3.1.1 Oxidoreductase	26

2.3.1.2	Isomerase .....	28
2.3.1.3	Ligandin .....	29
2.3.2	Classification .....	29
2.3.2.1	Cytosolic GST.....	30
2.3.2.2	Mitochondrial GST .....	31
2.3.2.3	MAPEG.....	31
2.4	Bacterial Glutathione S-Transferase .....	32
2.4.1	Special function of bacterial GST.....	33
2.4.1.1	Dehalogenase .....	33
2.4.1.1.1	Dichloromethane (DCM).....	33
2.4.1.1.2	Tetrachlorohydroquinone .....	34
2.4.1.1.3	Herbicides .....	35
2.4.1.2	Aromatic compounds catabolism.....	36
2.4.1.3	Isoprene catabolism .....	37
2.4.1.4	Lignin degradation .....	37
2.4.1.5	Antibiotics interaction.....	39
2.4.2	Cytosolic bacterial GST classification .....	39
2.4.2.1	Beta .....	39
2.4.2.2	Theta .....	40
2.4.2.3	Zeta .....	41
2.4.2.4	Chi.....	42
2.4.2.5	Eta .....	44
2.4.2.6	Rho.....	44
2.4.2.7	Nu.....	45
2.4.2.8	Xi.....	45
2.5	KKSG6 .....	46
<b>CHAPTER 3: METHODOLOGY .....</b>		<b>48</b>
3.1	Materials .....	48

3.1.1	Chemicals .....	48
3.1.2	Solutions .....	48
3.1.3	Instruments .....	49
3.1.4	<i>Escherichia coli</i> BL21 Star™ (DE3).....	49
3.1.5	pET101/D-TOPO®-KKSG6 .....	50
3.2	Methods .....	50
3.2.1	Bacteria retrieval.....	51
3.2.2	Bacterial validation.....	51
3.2.2.1	Plasmid size analysis.....	52
3.2.2.1.1	Plasmid extraction .....	52
3.2.2.1.2	Plasmid linearisation.....	52
3.2.2.2	Polymerase chain reaction .....	53
3.2.3	Agarose electrophoresis.....	54
3.2.4	Expression of KKSG6 .....	54
3.2.5	Optimisation expression of KKSG6 .....	55
3.2.5.1	Post-induction incubation time optimisation .....	55
3.2.5.2	IPTG concentration optimisation.....	55
3.2.6	Bacteria cell lysis.....	56
3.2.7	Protein purification .....	57
3.2.8	Sodium dodecyl sulfate-polyacrilamide gel electrophoresis .....	57
3.2.9	Glutathione S-transferase assay .....	58
3.2.10	Antibiotic susceptibility testing .....	58
3.2.11	Antibiotic conjugation study.....	59
3.2.12	Molecular docking.....	59
3.2.12.1	Structure prediction .....	60
3.2.12.2	Ligand structure preparation .....	60
3.2.12.3	Protein-ligand docking .....	60

<b>CHAPTER 4: RESULT .....</b>	<b>62</b>
4.1 Bacterial retrieval.....	62
4.2 Bacterial validation .....	62
4.2.1 Plasmid size analysis .....	62
4.2.2 PCR analysis.....	64
4.3 Expression of KKSG6.....	64
4.4 Optimisation expression of KKSG6 .....	64
4.5 Bacterial cell lysis .....	66
4.6 Protein purification .....	67
4.7 Antibiotic susceptibility testing .....	67
4.8 Antibiotic conjugation study.....	70
4.9 Molecular docking .....	71
4.9.1 Structure prediction .....	72
4.9.2 Protein-ligand docking.....	72
<b>CHAPTER 5: DISCUSSION.....</b>	<b>76</b>
5.1 Bacterial retrieval.....	76
5.2 Bacterial validation .....	76
5.2.1 Plasmid size analysis .....	77
5.2.2 PCR analysis.....	79
5.3 Expression of KKSG6.....	79
5.4 Optimisation expression of KKSG6 .....	80
5.5 Bacterial cell lysis .....	82
5.6 Protein purification .....	83
5.7 Antibiotic susceptibility testing .....	84
5.8 Antibiotic conjugation study.....	87
5.9 Molecular docking .....	89
5.9.1 Structure prediction .....	89
5.9.2 Protein-ligand docking.....	92

<b>CHAPTER 6: CONCLUSION .....</b>	<b>94</b>
6.1 Conclusion .....	94
6.2 Future work .....	94
<b>REFERENCES .....</b>	<b>96</b>
<b>APPENDICES .....</b>	<b>105</b>

Universiti Malaya

## LIST OF FIGURES

Figure 2.1	: Arsphenamine .....	18
Figure 2.2	: Structures of several antibiotics .....	21
Figure 2.3	: Horizontal gene transfer mechanisms .....	25
Figure 2.4	: Conjugation reaction mechanism between 1-chloro-2,4-dinitrobenzene and GSH.....	26
Figure 2.5	: Two steps reduction of lipid hydroperoxide .....	27
Figure 2.6	: Reduction of benzoquinone .....	28
Figure 2.7	: Isomerisation of 13-cis-retinoic acid to trans-retinoic acid .....	29
Figure 2.8	: Dehalogenation of DCM into formaldehyde .....	34
Figure 2.9	: Reductive dehalogenation of TCHQ.....	35
Figure 2.10	: Atrazine metabolism .....	35
Figure 2.11	: Organisation of <i>bph</i> operon in <i>Burkholderia xenovorans</i> LB400 (Fortin et al., 2006) .....	36
Figure 2.12	: Isoprene catabolism .....	37
Figure 2.13	: Lignin degradation process by ligE, ligF and ligG .....	38
Figure 2.14	: Amino acid sequence alignment of <i>Methylobacterium</i> sp. DM4 and <i>Methylophilus</i> sp. DM11 DCMD with the other theta class GST.....	41
Figure 2.15	: Naphthalene metabolism.....	42
Figure 2.16	: Amino acids alignment of KKSG6 and other members of beta class GST.....	47
Figure 3.1	: pET101/D-TOPO <sup>®</sup> -KKSG6.....	50
Figure 3.2	: Research workflow .....	51
Figure 3.3	: Polymerase chain reaction condition .....	54
Figure 3.4	: GSTrap <sup>™</sup> HP column principles .....	56
Figure 4.1	: Bacterial plate .....	62
Figure 4.2	: pET101/D-TOPO <sup>®</sup> -KKSG6 extraction electrophoregram .....	63

Figure 4.3	: pET101/D-TOPO <sup>®</sup> -KKSG6 size analysis electrophoregram .....	63
Figure 4.4	: PCR colony electrophoregram .....	64
Figure 4.5	: KKSG6 expression electrophoregram .....	65
Figure 4.6	: Effect of post-induction incubation time on KKSG6 expression .....	65
Figure 4.7	: Effect of IPTG concentration on KKSG6 expression.....	66
Figure 4.8	: Cell lysis electrophoregram .....	66
Figure 4.9	: Protein purification electrophoregram .....	67
Figure 4.10	: <i>E. coli</i> susceptibility towards kanamycin .....	68
Figure 4.11	: <i>E. coli</i> susceptibility towards streptomycin .....	68
Figure 4.12	: <i>E. coli</i> susceptibility towards gentamycin .....	69
Figure 4.13	: <i>E. coli</i> susceptibility towards tetracycline .....	69
Figure 4.14	: <i>E. coli</i> susceptibility towards chloramphenicol .....	70
Figure 4.15	: Thin layer chromatogram of antibiotic conjugate.....	71
Figure 4.16	: KKSG6 assay with and without chloramphenicol.....	71
Figure 4.17	: KKSG6 3D structure model.....	73
Figure 4.18	: Antibiotics binding within KKSG6 H-site.....	73
Figure 4.19	: Antibiotics binding within KKSG6 dimer interface .....	74
Figure 5.1	: Plasmid conformations .....	78
Figure 5.2	: Chloramphenicol, kanamycin and tetracycline structure comparison .....	89
Figure 5.3	: Docking sites.....	91

## LIST OF TABLES

Table 2.1 : Molecular target of various antibiotic classes (Source: Hutchings et al., (2019) with modifications).....	22
Table 2.2 : Distinguish properties between eukaryote and bacterial GST .....	32
Table 2.3 : Lignin composing monomers .....	38
Table 2.4 : Comparison of bacterial cytosolic GST classes.....	43
Table 2.5 : Identity percentage of KKSG6 with the other member of beta class GST ..	47
Table 3.1 : Solutions and their compositions .....	49
Table 3.2 : Linearisation reaction mixture .....	53
Table 3.3 : Polymerase chain reaction recipe.....	53
Table 3.4 : Polyacrylamide gel components .....	57
Table 3.5 : Glutathione S-transferase assay mixture.....	58
Table 3.6 : Antibiotics concentrations for serial dilution.....	59
Table 4.1 : Atom contacts and geometry analysis.....	72
Table 4.2 : KKSG6 interaction with antibiotics.....	75
Table 5.1 : Three types of cell lysis comparison.....	83
Table 5.2 : Comparison between comparative and ab-initio modelling .....	90

## LIST OF SYMBOLS AND ABBREVIATIONS

GST	: Glutathione S-Transferase
APS	: Ammonium persulfate
CDNB	: 1-Chloro-2,4-dinitrobenzene
DCM	: Dichloromethane
GSH	: Glutathione
IPTG	: Isopropyl $\beta$ - D-1-thiogalactopyranoside
MAPEG	: Membrane-associated proteins in eicosanoid and glutathione metabolism
MDR	Multidrug resistance
OD <sub>600</sub>	: Optical density at $\lambda = 600$ nm
PCB	: Polychlorinated biphenyl
PCR	: Polymerase chain reaction
ROS	: Reactive oxygen species
SDS-PAGE	: Sodium Dodecyl Sulphate-Polyacrylamide Gel Electrophoresis
TCHQ	: Tetrachlorohydroquinone
TEMED	: N,N,N',N'-tetramethylethane-1,2-diamine

## LIST OF APPENDICES

Appendix A: KKSG6 nucleic acid and amino acid sequence .....	105
Appendix B: Optimisation expression raw data .....	106
Appendix C: Antibiotic susceptibility raw data .....	108

Universiti Malaya

## CHAPTER 1:INTRODUCTION

### 1.1 General introduction

Antibiotic resistance is a phenomenon when bacteria develop mechanisms to defend themselves against drugs designed to kill them. As consequence, bacteria can no longer be effectively killed by the specific antibiotic, leading to higher medical costs and mortality. Antibiotic resistance is considered one of the most serious threats to global health. By 2050, antibiotic resistance is predicted to kill more than 10 million people annually if no meaningful action is taken (O'Neill, 2016). According to the Centers for Disease Control (2019), more than 2.8 million antibiotic-resistance infections occur in the United States each year, with more than 35,000 people die as a result. To suppress the antibiotic resistance growth and dissemination, multisectoral parties such as individuals, policy makers and health professionals must work together. However, preventing and controlling the resistance is merely to manage the resistance not to be worsen. Development of new antibiotics and novel alternatives for infectious diseases treatment could be the answer for this problem's long-term sustainability (Aminov, 2010; Bush et al., 2011; Frieri et al., 2017). Unfortunately, the understanding of antibiotic resistance mechanism which might be important in developing effective antibiotics and their alternatives is still poorly understood.

Glutathione S-transferase (GST) is an enzyme that involve in detoxification process. This enzyme eliminates xenobiotic compounds from the cells by conjugating them with glutathione, creating the more water-soluble molecule that can be further metabolised and secreted out from the cells. Despite facilitating the organisms to survive under xenobiotic stress, GST activity is also known to be correlated with drug resistance phenomenon. Within bacterial cells, cytosolic beta class GST is known to involve in antibiotic

resistance development. The study of antibiotic resistance mechanism developed by beta class GST will be the main focus of this research.

## **1.2 Problem statement**

The role of beta class GST in the antibiotic resistance was initially proposed during the study of *Proteus mirabilis* GST isozyme (PmGST B1-1). The presence of PmGST B1-1 in *Escherichia coli* culture was reported to reduce bacterial cells' susceptibility towards several antibiotics (Allocati et al., 1999). This phenomenon was intriguingly specific for beta class GST, since no susceptibility difference observed when the same experiment was conducted towards mammalian GST. The involvement of beta class GST in protecting bacterial cells against antibiotics was also supported by the fact that PmGST B1-1 is mainly found in periplasmic space rather than in cytosol (Allocati et al., 1994).

So far, studies of beta class GST interaction with antibiotics have mainly been conducted using PmGST B1-1 and limited only to a few antibiotics. Whether other beta class GSTs exhibit the same activity towards different classes of antibiotics remains unknown.

## **1.3 Objectives**

In this research, the study of antibiotic resistance developed by beta class GST was conducted using KKSG6, one of GST isozymes found in *Acidovorax* sp. KKS102. Therefore, the objectives of this study are: a) to express and purify recombinant GST isoform KKSG6, b) to determine the antibiotic susceptibility of *E. coli* harbouring KKSG6 gene, and c) to evaluate the binding behaviour of the antibiotics on the GST isozyme.

## CHAPTER 2: LITERATURE REVIEW

### 2.1 Antibiotics

Antibiotics were initially defined as molecules that microorganisms produce to kill competing bacteria. However, it has been generalised to include other synthetic chemicals. Antibiotics are widely used as a treatment for bacterial infection diseases, such as tuberculosis, pneumonia and gonorrhoea. The very first antibiotic, arsphenamine, was developed in 1909 by Paul Ehrlich and proven to be effective in treating syphilis (Gould, 2016). The invention of this arsenic-based chemical then popularised the concept of ‘magic bullet’ which refers to a specific-targeted drug. The structure of arsphenamine is given in **Figure 2.1**.

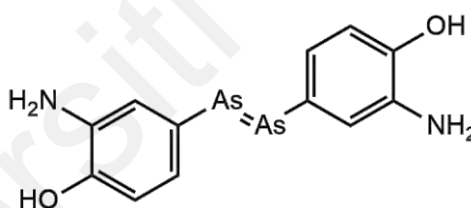


**Figure 2.1: Arsphenamine**

In 1928, penicillin was discovered when Alexander Fleming accidentally found that a fungus belonging to the *Penicillium* genus could kill *Staphylococcus* and other gram-positive bacteria. The presence of naturally produced antibiotics within microorganisms is known to act as a chemical weapon to kill competitors. Since then, extensive research into antibiotics sourced from microorganism metabolites has been conducted. It was then explained why the majority of the antibiotics available today come from the natural

products of microorganisms. Even synthetic antibiotics principally mimic the natural metabolites.

### **2.1.1 Mechanisms**

Basically, antibiotics work by disrupting or blocking the compound or process necessary for bacterial survival. The following subsections explain the mechanisms of how antibiotics can kill or inhibit the growth of bacterial cells. The molecular structure of several antibiotics mentioned below are provided in **Figure 2.2**.

#### **2.1.1.1 Cell wall synthesis inhibition**

The cell wall is an essential component of bacterial cells. It maintains all cell contents together and protects them from the outer environment. Penicillin is one of antibiotics that inhibits cell wall synthesis. It irreversibly binds to DD-Transpeptidases, the enzyme which responsible for peptidoglycan cross-linking to the cell wall and blocks its activity (Frère et al., 1984). As a result, gram-negative bacteria whose the cell wall is primarily constituted by peptidoglycan cannot survive while being treated with this antibiotic. On the other hand, human cells that lack a cell wall will be unaffected by the drug.

#### **2.1.1.2 Protein synthesis inhibition**

Tetracycline is one of the antibiotics that acts as a protein synthesis inhibitor. Discovered in the 1940s, tetracycline is known to bind with 30S ribosomal subunit of bacteria, resulting the elongation process of protein biosynthesis to halt due to a lack of aminoacyl-tRNA attachment to ribosomal complex (Chopra & Roberts, 2001). Aside from bacterial infections, this drug has been known to be used in *Plasmodium* parasites infections by inhibiting the activity of the 70S complex within mitochondria (Dahl et al.,

2006). This inhibition then impairs expression of apicoplast, which is essential for parasite survival. Since the drug has low affinity towards mammalian 80S ribosomes, it acts specifically on the 70S ribosomes-harboring cells.

#### **2.1.1.3 DNA synthesis inhibition**

DNA replication is a critical step in the cell duplication process. Prior to cell duplication, the genetic material of the parent cell requires to be copied to be used as a blueprint of the new cell. Some antibiotics, such as ciprofloxacin and metronidazole, are targeting the DNA synthesis process to prevent bacterial duplication. Ciprofloxacin inhibits bacterial DNA topoisomerase which is responsible for super coil relaxation (Thai et al., 2021). Within the cells, DNA replication is initiated by the alteration of super-coiled DNA into a more relaxed three-dimensional conformation to allow DNA polymerase to access the origin of replication. As a consequence, inhibiting DNA topoisomerase activity will prevent overall DNA replication which is further implicated in cell duplication inhibition.

#### **2.1.1.4 RNA synthesis inhibition**

Rifampicin is an antibiotic that works by inhibiting bacterial cell RNA synthesis. Binding of rifampicin to DNA-dependent RNA polymerase will block RNA elongation, which further leads to the lack of protein expression (Campbell et al., 2001). Since proteins have various important functions, inhibiting protein production means halting all biological processes within the bacterial cell. The specificity of rifampicin is derived from the drug's specific binding to bacterial RNA polymerase. Thus, mammalian RNA polymerase is necessarily unaffected by the drug.

### 2.1.1.5 Folic acid synthesis inhibition

Within the cells, folic acid is essential for protein and nucleic acid biosynthesis. Under normal conditions, dihydropteroate synthase (DHPS) converts para-amino-benzoic acid (PABA) to dihydropteroic acid, the precursor of folic acid. However, due to the structure similarity between antibiotic sulfadiazine and BAPA, the drug's presence will competitively inhibit the binding of DHPS and BAPA (Capasso & Supuran, 2014). DHPS itself is known to be found only in prokaryote cells or other simple organisms. The absence of DHPS in mammals is rationalised by the fact that, rather than synthesising folic acid in the body, mammals obtain it from dietary.

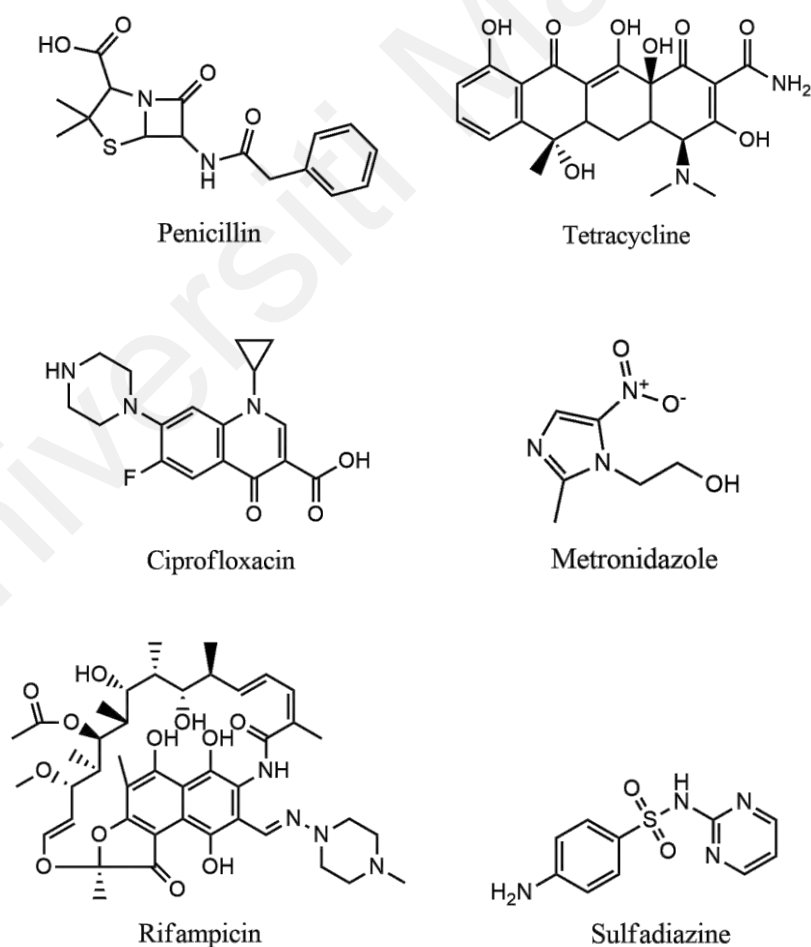


**Figure 2.2: Structures of several antibiotics**

### 2.1.2 Classification

Antibiotics are grouped based on their structural similarities and mechanisms. Several classes of antibiotics and their molecular targets are given in **Table 2.1**.

**Table 2.1: Molecular target of various antibiotic classes (Source: Hutchings et al., (2019) with modifications)**

Mechanism	Class	Example	Molecular target
Cell wall synthesis inhibition	$\beta$ -lactams	Amoxilin, cefalexin	Penicillin-binding proteins inhibition
	Cycloserines	Seromycin	Alanine racemase and D-alanine-D-alanine ligase inhibition
	Phosphonates	Fosfomycin	MurA inhibition
	Thioamides	Ethionamide	Mycolic acid synthesis inhibition
	Carbapenems	Meropenem, doripenem, ertapenem	Penicillin-binding proteins inhibition
	Lipopeptides	Daptomycin, surfactin	Cell wall disruption
Protein synthesis inhibition	Aminoglycosides	Kanamycin A, streptomycin, gentamycin	30S ribosome subunit inhibition
	Tetracyclines	Tetracycline, anhydrotetracycline, doxycycline	
	Amphenicols	Chloramphenicol	50S ribosome subunit inhibition
	Streptogramins	Pristinamycin, dalfopristin	
DNA synthesis inhibition	Flouroquinolones	Ciprofloxacin, levofloxacin	DNA topoisomerase inhibition
	Nitrofurans	Nitrofurantoin	DNA damage
	Phenazines	Clofazimine	Binds to guanine bases
RNA synthesis inhibition	Ansamycins	Rifamycin, rifamycin SV	RNA polymerase
Folic acid synthesis inhibition	Sulfonamides	Mafenide, sulfadiazine, protosil	Dihydropteroate synthetase inhibition
	Diaminopyrimidines	Trimethoprim	

## 2.2 Antibiotic resistance

Antibiotic resistance occurs when bacteria develop defence mechanisms against drugs designed to kill them. As a result, bacterial infection diseases are becoming more difficult to treat as the antibiotics become less effective. Bacterial cells naturally evolve resistance through random mutation as part of the adaptation process for natural selection (Maclean et al., 2010). However, antibiotics misuse in humans and animals speeds up the process.

### 2.2.1 Current status

Antibiotic resistance has been observed for nearly one century since the early days of antibiotic use. The first antibiotic resistant was reported even before penicillin was discovered (Stekel, 2018). In 1924, it was revealed that bacterial resistance towards Salvarsan, the medication used to treat syphilis, had been emerged. Luckily, many new antibiotics were introduced during that period, providing alternative treatments so that the effect of antibiotic resistance can be suppressed. In the present day, antibiotic resistance is considered being in the critical status due to the emergence of antibiotic resistance and lack of new antibiotics discoveries.

Nowadays, many bacterial pathogens have acquired multidrug resistance (MDR) due to inappropriate antibiotic usage. The microorganisms, including bacteria, that are resistance to most antibiotics or other drugs used to treat infectious diseases are commonly referred to as superbugs (Davies & Davies, 2010). Their genetic material is known to have multiple mutations, allowing them to own high resistance towards various antibiotic classes. *Pseudomonas aeruginosa*, *Acinetobacter baumannii*, *Escherichia coli*, *Klebsiella pneumoniae*, *Staphylococcus aureus* and *Mycobacterium tuberculosis* are some pathogen bacteria that have been reported to develop MDR (Khan & Khan, 2016). MDR bacterial pathogens are usually treated with carbapenem, the antibiotic which belongs to the  $\beta$ -lactam class, as a last ultimate option for bacterial infection (Elshamy &

Aboshanab, 2020). The resistance against carbapenem was expected to develop much slower due to its resistance towards  $\beta$ -lactamases hydrolysis. However, the carbapenem resistance has still yet been reported in various Enterobacteriaceae family (Papp-Wallace et al., 2011). It then makes the current status of antibiotic resistance threat more serious. Without urgent actions, we might go back to the pre-antibiotics dark ages.

### 2.2.2 Mechanisms and origin

Bacterial cells develop resistance towards antibiotics through a variety of mechanisms: cell wall permeability change that prevents drugs to get into target sites, active efflux towards antibiotics, modification of antibiotics inside the cells, degradation of antibiotics, establishment of alternative drug-inhibited pathways, target modification and target overexpression (van Hoek et al., 2011). Those are acquired from random mutation and gene transfer. Random mutations naturally occur within bacterial cells during the replication process. It can also be induced by environmental exposure, including antibiotics. Antibiotics have been manufactured, utilised and released into the ecosystem for over half century. Not only for clinical purposes, but antibiotics are also commonly use in animal husbandry and agriculture (Tripathi & Cytryn, 2017). The widely disseminated antibiotics in biosphere due to anthropogenic activity allows continuous selection and force bacteria to adapt in that environment (Aminov, 2009). Horizontal gene transfer also plays a role in antibiotic resistance transmission (Burmeister, 2015). Bacterial cells are known to acquire resistance through three mechanisms: a) transformation, the direct pull of short genetic fragments from the environment, b) conjugation, genetic material swap via sexual pilus, and c) transduction, bacteriophage-mediated genetic exchange (see **Figure 2.3**) (Sun, 2018).

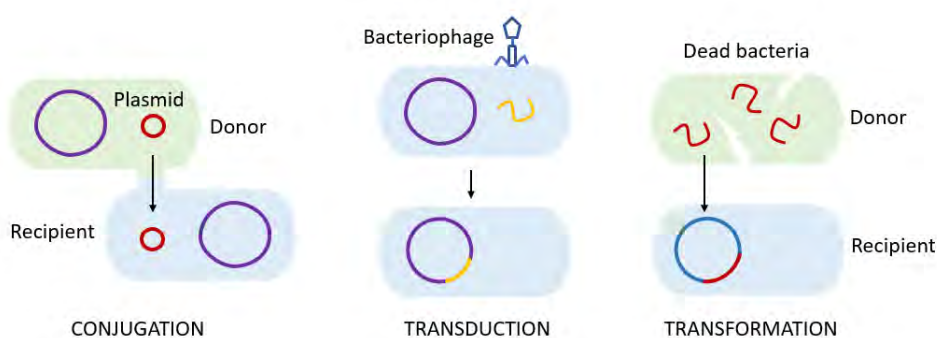


**Figure 2.3: Horizontal gene transfer mechanisms**

### 2.3 Glutathione S-transferase

Glutathione S-Transferase (EC 2.5.1.18, GST) is the ancient enzyme superfamily that found is in most aerobic organisms, including mammals, birds, insects, fish, plants and bacteria (Sherratt & Hayes, 2002). This enzyme family is known to have an important role in the intracellular detoxification process (Dasari, 2017; Jakoby & Keen, 1977). GST catalyses the conjugation reaction between the electrophilic compounds and the reduced form of glutathione (GSH) through the nucleophilic substitution mechanism. The reaction starts with the activation of the GSH thiol group by forming a  $GS^-$  ion and then proceeds with the nucleophilic attack (Angelucci et al., 2005). **Figure 2.4** is the mechanism reaction of the conjugation reaction which is catalysed by GST.

In general, the conjugation reaction which catalyse by GST intend to alter non-polar toxic agents into more water-soluble substances, so it can be further metabolised and excreted out from the cells actively through some excretion mechanism (Allocati et al., 2009; Sheehan et al., 2001).

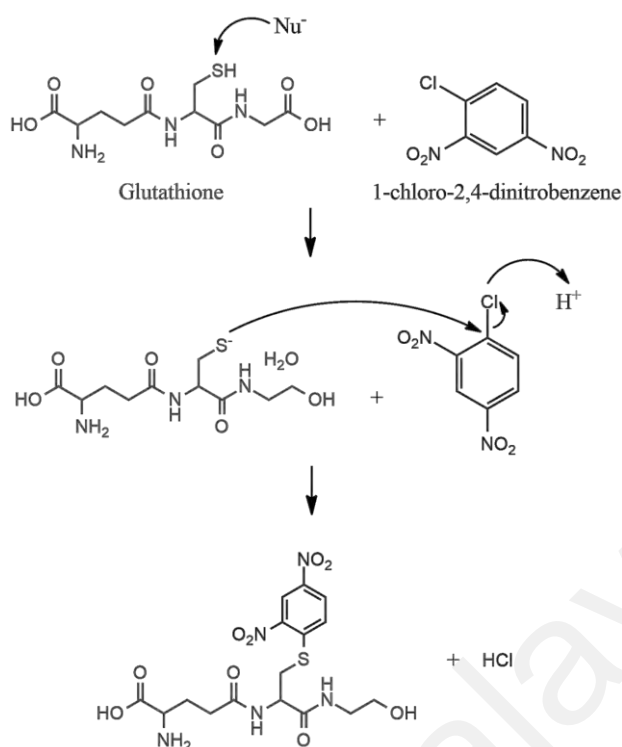


**Figure 2.4: Conjugation reaction mechanism between 1-chloro-2,4-dinitrobenzene and GSH**

### 2.3.1 Functions of GST

Besides catalysing the conjugation reaction between GSH and hydrophobic molecules, other GSH-dependant reactions such as oxidoreduction and isomerisation are also observed to be catalysed by GST family (Chen & Juchau, 1997; Sharma et al., 2004). GST also exhibits several non-catalytic functions such as sequestration with reactive compounds, intracellular transport of non-polar molecules and signal transduction regulation (Jakoby & Keen, 1977; Pajaud et al., 2012). Here are summarised several functions of GST.

#### 2.3.1.1 Oxidoreductase

The reduction of lipid hydroperoxide is one of GSH-dependant reaction which catalysed by GST. Along with the aerobic metabolism processes, reactive oxygen species

(ROS) such as  $\text{H}_2\text{O}_2$ ,  $\text{O}_2^{\cdot-}$  and  $\text{OH}^\cdot$  will definitely generated within the cells due to partial reduction of  $\text{O}_2$  (Hossain et al., 2006). These reactive ROS can easily interact with the macromolecule including DNA, protein and lipid. Reaction between ROS and lipid will cause the oxidative degradation of the lipid itself. As consequence, several harmful molecules such as lipid hydroperoxides, malondialdehydes and 4-hydroxyalkenals will be formed. Under the physiological or low lipid peroxides concentration, the cells will protect themselves through antioxidant defence systems. If the defence systems cannot overcome the oxidative damage, the cell will trigger apoptosis (Ayala et al., 2014). By undergoing the reduction of lipid hydroperoxides to another less harmful molecules, GST can prevent the cell death due to high oxidative stress (Raza, 2011). **Figure 2.5** is the lipid hydroperoxide reduction reaction catalysed by GST. The reduction occurs in two-step reactions. The first step is an enzymatic reaction which alter peroxide group into alcohol group that will form GS-OH as a by-product. GS-OH then undergoes the spontaneous reaction with GSH to form water and oxidised form of glutathione (GS-SG).

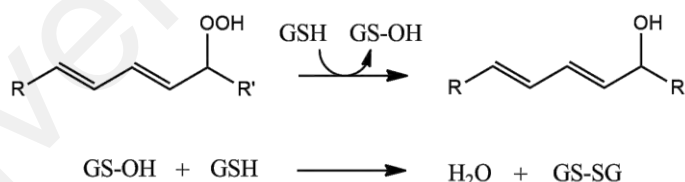


**Figure 2.5: Two steps reduction of lipid hydroperoxide**

Besides acting as a GSH-dependent hydroperoxidase, GST also exhibit GSH-dependent reductase activity towards glutathionyl-hydroquinone (GS-hydroquinone). Glutathionyl-hydroquinone reductase (GS-HQR) was first found in a pentachlorophenol (PCP) degrader microorganism, *Sphingobium chlorophenolicum* ATCC 39723 (Belchik & Xun, 2011). GS-HQR within *S. chlorophenolicum* (PcpF) was observed to play an

important role to maintain the concentration of hydroquinone, a metabolic intermediate of (PCP) (Huang et al., 2008). Within the cells, hydroquinone will be automatically oxidised to benzoquinone. With the presence of GSH, benzoquinone then spontaneously undergo the Michael's addition reaction, forming GS-hydroquinone. GS-HQR then converts GS-hydroquinone back to hydroquinone (see **Figure 2.6**).

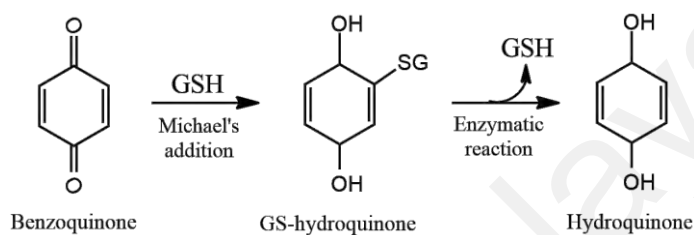


**Figure 2.6: Reduction of benzoquinone**

#### 2.3.1.2 Isomerase

In signaling pathway, retinoic acid plays a necessary role to regulate several biological processes by interacting with nuclear retinoic acid receptors. The interaction between retinoic acid and receptors then lead to either the upregulating or repressing the certain genes transcription (Das et al., 2014). Due to the presence of several conjugation unsaturated carbons, retinoic acids are unstable and susceptible against oxidation and isomerisation reactions. Therefore, within the cells retinoic acid presence in several isomer including 13-*cis*-retinoic acid and all-*trans*-retinoic acid. Unfortunately, the interaction between each isomer with retinoic acid receptors exhibits the different binding affinity. 13-*cis*-retinoic acid is reported to have an extremely low affinity bindings to retinoic acid receptors and doesn't seem to undergo the signal transduction pathway (Tsukada et al., 2000). As consequence, it can lead to the several cell development problems and diseases. Hepatic GST from rat was reported to catalyse the isomerisation

of 13-*cis*-retinoic acid to all-*trans*-retinoic acid as presented in **Figure 2.7**. This isomerisation reaction is considered as a potential therapeutic activities to treat certain types of diseases.

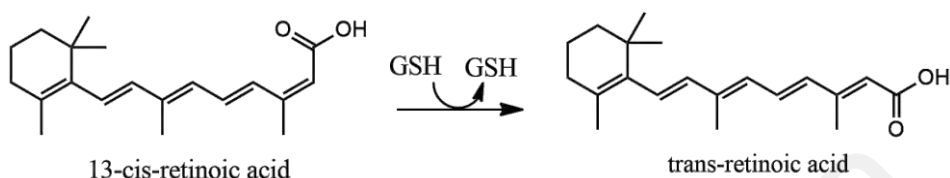


**Figure 2.7: Isomerisation of 13-*cis*-retinoic acid to trans-retinoic acid**

### 2.3.1.3 Ligandin

Ligandin is a term that used to refer the protein that possess the affinity against a broad range of ligands. In addition of its main function in catalysing the conjugation reaction, GST is also found to bind with various non-substrate hydrophobic compound (Axarli et al., 2004). Within the hepatic cells, GST proteins are observed to bind with bilirubin, carcinogens and steroids (Litwack et al., 1971). It then leads to the suggestion that GST involve in storage and transportation of several molecules (Martínez-Márquez et al., 2017; Turella et al., 2003). In the certain conditions, GST can also sacrifice themselves to undergoes the covalent interaction with reactive molecule in order to prevent the interaction between carcinogen and DNA (Brown & Gandolfi, 1994; Mitchell et al., 1995).

### 2.3.2 Classification

Based on their localisation in the cells, GSTs are classified into three different families 1) cytosolic 2) mitochondrial and 3) microsomal, which designated as membrane-

associated proteins in eicosanoid and glutathione metabolism (MAPEG) (Wikteliu & Stenberg, 2007). These three families are then sub-grouped into several sub-families or classes based on their amino acid sequence, three-dimensional structure, immunological and kinetics properties. The proteins that shares more than 40% sequence identity are grouped into the same class, while the proteins in the different class shares below 25% sequence identity (Allocati et al., 2009).

#### **2.3.2.1 Cytosolic GST**

Cytosolic GST constitute the largest class of the GST family. It can be rationalised by the fact that up to 90% of cellular GSH presents in the cytosol (Lu, 2009). All member of cytosolic GST present as soluble dimeric proteins. The dimer itself usually formed by the identical protein. However, heterodimeric protein which consist of two different monomers are also observed (Kontur et al., 2019). The monomer which constructs the cGST consist of two different domains, namely N-terminal and C-terminal. The active site that contributes in GSH binding (G-site) is located within N-terminal domain. G-site has also been implicated to the conserve amino acid sequence within this region. In the other hand, the C-terminal domain which consist of hydrophobic electrophile binding site (H-site) vary in the amino acid sequences (Dourado et al., 2008). The presence of variable amino acid sequences within H-site is directly related to the unspecific binding interactions. As one of the consequences, GST can bind with a broad range of hydrophobic molecules. Cytosolic GSTs are sub-grouped into at least thirteen classes: alpha, mu, pi, theta, sigma, zeta, omega, gamma, beta, chi, tau, delta and epsilon.

### **2.3.2.2 Mitochondrial GST**

Although most of GST presents in cytosol, it can also be found in mitochondria. The presence of this enzyme in mitochondria is strongly related with the function of GST as a defence system against ROS. Mitochondrial GST constitute their own subfamily which called kappa class. Unlike the other class of GST, kappa family proteins possess the cleavable mitochondria targeting signal (Raza, 2011). The rat GST subunit 13, rGSTK1, was the first protein which sub-grouped into this class (Pemble et al., 1996). rGSTK1 was previously classified into theta class. Nonetheless, it shares low sequence similarity with GSTs that belong to that class. Furthermore, rGSTK1 does not have the SNAIL/TRAIL (Ser-Asp-Ala-Ile-Leu/Thr-Arg/Ala-Ile-Leu) motif sequence that is usually possessed by the other classes. The absence of the SNAIL/TRAIL motif sequence within the N domain of the GST then become the identity of mitochondrial GST kappa class (Sheehan et al., 2001).

### **2.3.2.3 MAPEG**

Compared with cytosolic and mitochondrial GSTs, MAPEG presents a very different properties in structure and size. This class consist of integral membrane proteins that are not evolutionary related with other class of GST. However, just like the other GST, it reacts with the CDNB to undergo the conjugation reaction. The discovery of MAPEG family initially began with the finding of unique function of microsomal GST where the conjugation activity of this enzyme increase due to covalent modification (Morgenstern et al., 1979). MAPEG itself are sub-classified into several subgroups, namely MAPEG 1, MAPEG 2, MAPEG 3, 5-lipoxygenase activating protein (FLAP), leukotriene C<sub>4</sub> synthase (LTC<sub>4</sub>) and prostaglandin E synthase (PGES) (Muleta, 2016). MAPEG1 is the first protein in this class which the structure was solved. Generally, MAPEG presents as

a homotrimeric protein which the active site located at the subunit interface (Morgenstern et al., 2011).

## 2.4 Bacterial Glutathione S-Transferase

GST not only can be found in higher eukaryote organisms but also in single prokaryote bacterial cells. The occurrence of GST in bacteria initially known from the discovery of GSH S-transferase activity within *Escherichia coli* and *Xanthomonas oryzae* (Shishido, 1981). Compared to other eukaryote GSTs, bacterial GSTs exhibit several different properties which are summarised in **Table 2.2**. To date, within the bacteria kingdom, the existence of GST has been observed in proteobacteria (Santos et al., 2002), cyanobacteria (Wikteliuss & Stenberg, 2007), and gram-positive bacteria (Allocati et al., 2012).

**Table 2.2: Distinguish properties between eukaryote and bacterial GST**

No	Distinguishing Factor	Eukaryote GST	Microbial GST
1	Role in metabolism	Inactivation, degradation, and excretion hazardous molecules	Catabolic enzyme in primary metabolism: Promote the growth on recalcitrant molecules
2	Substrate specificity	Broad	Narrow
3	Activity towards CDNB	High	Low
4	Binding with GST column	Yes	No

Eukaryote GSTs usually play a role in inactivation, degradation and excretion of hazardous molecules. It also can be characterised by its activity towards CDNB and the ability to bind with GST affinity column. However, most of bacterial GSTs undergo the conjugation activity to promote the growth on recalcitrant molecules as a primary

metabolism process. It is then implicated to the specificity of bacterial GSTs towards only one substrate (S. Vuilleumier & Pagni, 2002). Unlike the eukaryote GSTs, bacterial GSTs usually show the low conjugation activity towards CDNB and cannot bind with the GST affinity column which also been correlated with the small number of bacterial GST which has been identified prior to the advent of large-scale genome sequencing.

#### **2.4.1 Special function of bacterial GST**

Within bacteria, the catalysis activity of GST implicated in the variety metabolic processes due to their ability to bind with a lot of substrates. Bacterial GSTs play a role in hydrolysis of dichloromethane, reductive dehalogenation of 2,3,5,6-tetrachloro-p-hydroquinone and opening the epoxide ring of 2,3-dichlorooxirane (Vuilleumier, 1997). They also take part in degradation of aromatic molecules and other hazardous chemicals including antibiotics. Here are summarised functions which have been observed in bacterial GST.

##### **2.4.1.1 Dehalogenase**

Halogenated molecules are widely used in manufacturing and have become a serious environmental issue. One of promising solution for this problem is bioremediation by using microorganism which possesses dehalogenase activity. Bacterial GST is observed to exhibit dehalogenase activity towards halogenated compounds, including aliphatic and aromatic molecules.

##### **2.4.1.1.1 Dichloromethane (DCM)**

Dichloromethane dehalogenase (DCMD) presents in some methylotrophic bacteria as a GSH-dependent enzyme. DCMD is used to alter DCM into formaldehyde as the initial

process of catabolism as in **Figure 2.8**. Formaldehyde that is produced from dehalogenation reaction then further catabolised to be used as a carbon source (Evans et al., 2000). While the reaction occurs, GSH cofactor will be regenerated as an intact molecule and is not incorporated with the reaction product (Kayser & Vuilleumier, 2001). The well-studied DCMD from *Methylobacterium* sp. DM4 and *Methylophilus* sp. DM11 exhibit close phylogenetic relation with theta class of GST. These enzymes possess the conserve serine residue within N-terminal domain which is one of the characteristics of theta class. However, these two enzymes do not exhibit the conjugation reaction towards DCNB and cannot bind to the GSH affinity column (Shehu et al., 2019).



**Figure 2.8: Dehalogenation of DCM into formaldehyde**

#### 2.4.1.1.2 Tetrachlorohydroquinone

Tetrachlorohydroquinone (TCHQ) dehalogenase is an enzyme that catalyse the reductive dehalogenation of TCHQ to trichlorohydroquinone and then to dichlorohydroquinone as in **Figure 2.9**. This enzyme was initially found in pentachlorophenol degradation pathway within soil bacteria *Spingobium chlorophenolicum* (Kiefer et al., 2002). TCHQ dehalogenase requires two molecules of GSH to remove a single chlorine atom from TCHQ. Dehalogenation process conducts in two steps. First, the enzyme catalyses the conjugation reaction between GSH and TCHQ. Other GSH molecule then form the disulphide bond with the previous conjugated GSH

with the help of cysteine residue within the TCHQ dehalogenase, forming the trichlorohydroquinone and oxidised form of glutathione (McCarthy et al., 1997).

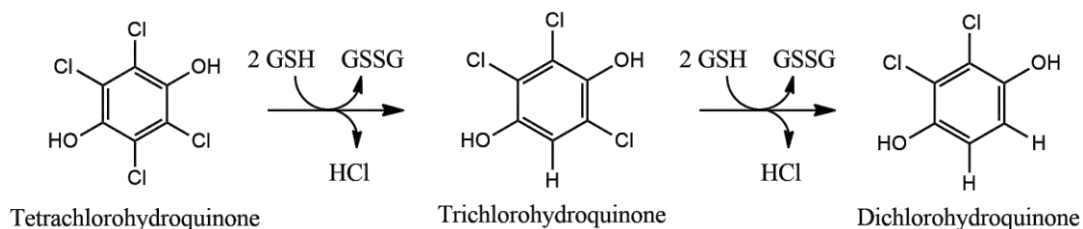


**Figure 2.9: Reductive dehalogenation of TCHQ**

#### 2.4.1.1.3 Herbicides

GSTs that found within rhizosphere microorganisms are known to have the ability to detoxify several types of herbicides, including atrazine and alachlor. *Pseudomonas* ADP and *Ochrobactrum anthropic* are two bacteria which observed to degrade atrazine. GSTs within those bacteria are believed to involve in the first step of atrazine catabolism by undergoing the GSH-dependent chlorine atom removal as in **Figure 2.10**. The detoxification process then proceed with the dealkylation of isopropylamine and ethylamine groups of atrazine-GSH conjugate (Allocati et al., 2009).

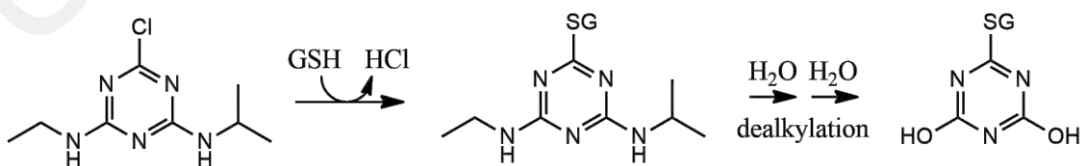


**Figure 2.10: Atrazine metabolism**

Two GSTs that belongs to *Pseudomonas flourences* BD4-13 and *Pseudomonas putida* M-17 has been reported to have the dechlorination activity towards alachlor. Unlike the atrazine catabolism, after the conjugation of GSH-herbicide formed, detoxification process proceed with hydrolysis by carboxypeptidase forming cysteine conjugate (Zablotowicz et al., 1995).

#### 2.4.1.2 Aromatic compounds catabolism

DNA sequence analysis towards some bacteria shows that GST genes present in the vicinity of aromatic molecule catabolism operon. It then rationalised the fact that GST also plays a role in degrading aromatic compounds. The most well-known GST gene in *Burkholderia xenovorans* LB400, BphK, is known to involve in degradation of aromatic compound biphenyl/polychlorinated biphenyl (Lloyd-Jones & Lau, 1997). The organisation of *bph* operon, the regulatory system of gene cluster that promote the catabolism of biphenyl/polychlorinated biphenyl, within *Burkholderia xenovorans* LB400 can be seen in **Figure 2.11**. Another BphK homologue with 61% amino acid sequence identity, XylK, was also seemed to be involve in toluene and xylene degradation pathway within *Cycloclasticus oligotrophus* RB1 (Wang et al., 2009). Although the exact physiological role and the specific substrate of XylK remain unknown, it exhibits the activity towards aromatic molecule CDNB.



**Figure 2.11: Organisation of *bph* operon in *Burkholderia xenovorans* LB400** (Fortin et al., 2006)

### 2.4.1.3 Isoprene catabolism

Two GSTs within *Rhodococcus* sp. AD45 are observed to be involved in isoprene degradation process. The first GST, *isoI*, catalyses the opening of 3,4-epoxy-3-methyl-1-butene epoxide ring to form 1-hydroxy-2-glutathionyl-2-methyl-3-butene. This GSH conjugate then undergoes the two steps oxidation process into 2-glutathionyl-2-methyl-3-butenic acid (van Hylckama Vlieg et al., 1999). Further metabolic process of this molecule remains unknown. However, this molecule is hypothesised to undergo the conjugation reaction with CoA group and then proceed with GSH removal by the second GST, *isoJ* (Van Hylckama Vlieg et al., 2000). The brief metabolism of isoprene can be seen in **Figure 2.12**.

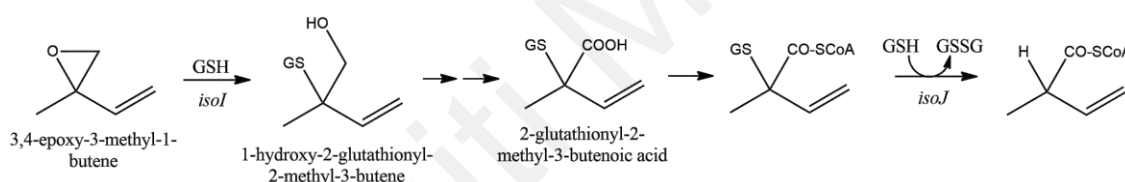


**Figure 2.12: Isoprene catabolism**

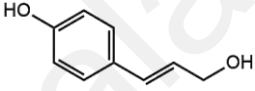
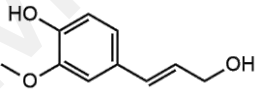
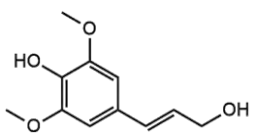
### 2.4.1.4 Lignin degradation

Lignin is an irregular biopolymer which composed of three molecules, namely p-coumaryl alcohol, coniferyl alcohol and sinapyl alcohol (see **Table 2.3**). The occurrence of lignin on Earth is abundant and its degradation by the microorganisms become an important step of carbon cycle. Bacterial GST has been known to involve in this process.

Within soil bacterium *Sphingomonas* sp. SYK-6, there are total three GSTs which promote degradation of lignin, each are encoded by *ligE*, *ligF* and *ligG* (Meux et al., 2011). Both *ligE* and *ligF* play a role in the breakdown of  $\beta$ -aryl ether, the most abundance intramolecular bond presence within the lignin (Masai et al., 2003). Those two enzymes

are enantiospecific. *LigE* and *ligF* only can cleave the  $\beta$ -aryl ether successively with the (*R*) and (*S*)-stereoisomer (Kontur et al., 2018). Meanwhile, *ligG* have a role to eliminate GSH molecule which has been previously conjugated with lignin as a final step of degradation process. The reaction of lignin degradation process by *ligE*, *ligF* and *ligG* can be seen in **Figure 2.13**.

**Table 2.3: Lignin composing monomers**

Lignin monomer	Structure
p-coumaryl alcohol	
Coniferyl alcohol	
Sinapyl alcohol	

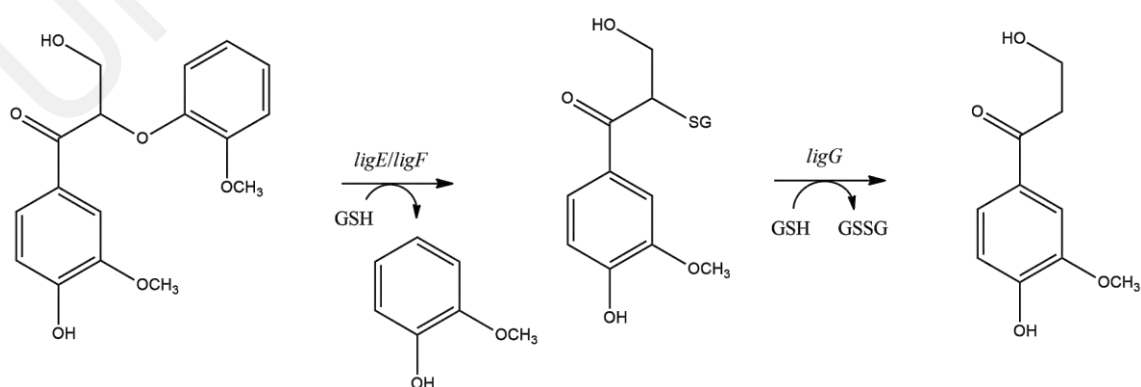


**Figure 2.13: Lignin degradation process by *ligE*, *ligF* and *ligG***

#### 2.4.1.5 Antibiotics interaction

As previously explain in 2.3.1.3, GST can also act as a ligandin. It can bind with several toxic molecules, including antibiotics. The *in vitro* studies towards *Proteus mirabilis* GST (PmGST) using mammalian GSTs as the control has shown that bacterial GST diminish the activity of some antibiotics. The minimum inhibitory concentration for amikacin, ampicillin, cefotaxime, cephalothin and nalidixic acid was increased by the presence of PmGST (Piccolomini et al., 1989). Reverse genetic study has also shown that under phosphomycin treatment, higher viability of wild type *P. mirabilis* observed compared with engineered GST-devoid *P. mirabilis* (Allocati et al., 2003).

#### 2.4.2 Cytosolic bacterial GST classification

Bacterial GSTs are currently known to be classified into four classes: cytosolic, mitochondrial, microsomal and bacterial-specific fosfomycin-resistance protein. The cytosolic bacterial GST then regrouped into at least eight classes: beta, theta, zeta, chi, eta, rho, nu and xi. The comparison between those classes is summarized in **Table 2.4**.

##### 2.4.2.1 Beta

Beta class was initially discovered by the characterisation of *Proteus mirabilis* GST (GSTB1-1). Immunological study revealed that GSTB1-1 was unrecognised by mammalian antisera, denoting the structural distinction with mammalian GST (Di Illo et al., 1988). It was also observed that the amino acid sequence of GSTB1-1 differs from other classes (Mignogna et al., 1993). The completion of GSTB1-1 3D structure unveiled the presence of mixed disulfide bond within its active site which has not been observed in other GST classes (Rossjohn et al., 1998). The presence of conserve cysteine residue within GSH binding domain then become the identity of the beta class (Federici et al.,

2010). Since this GST class was first identified within bacteria, the name of the class was chosen after the organism which it originated. To date, there is no non-bacterial GST has been grouped into this class, making it as a bacteria-specific GST class.

Compared to the theta class, the class which most of beta class members were originally classified, dimer interphase of beta class is closed pack and dominated by the polar interaction. Meanwhile, dimer interphase of theta class is way more open and dominated by hydrophobic residue (Sheehan et al., 2001).

#### 2.4.2.2 Theta

Bacterial cytosolic theta class is specific for methylotrophic bacteria such as *Methylobacterium* sp. DM4 (La Roche & Leisinger, 1991), *Methylophilus* sp. DM11 (Bader & Leisinger, 1994a), *Hyphomicrobium* sp. DM2 (Kohler-Staub & Leisinger, 1985) and *Methylophilus* sp. DM13 (Doronina et al., 1995). As previously mention in 2.4.1.1.1, bacterial theta class GSTs possess the DCMD activity to catabolise the single carbon molecule DCM as a carbon source. Amino acid sequence analysis of both *Methylobacterium* sp. DM4 and *Methylophilus* sp. DM1 from *dcmA* gene shown that these two GSTs are more closely related with eukaryote theta class than to other bacterial GSTs (Bader & Leisinger, 1994b).

Moreover, highly conserved Ser-9 which is essential in catalytic mechanism of theta class GST is observed within these two DCMD proteins (see **Figure 2.14**) (P. G. Board et al., 1995; Caccuri et al., 1997). The evidence is also supported by the fact that, just like the other eukaryote theta class GSTs, these two GSTs are also unable to bind with the GSH-affinity column and do not exhibit any activity towards CDNB.

Methylobacterium	MSPNPTNIHTGKTLRLLYHPASQPCRSAHQFMYEIDVPFEEVVVDISTDITERQEFRDKY	60
Methylophilus	-----MSTKRLYLHHPASQPCRAVHQFMLENNIEFQEEIVDITTDINEQPEFRERY	51
Musca	-----MDFYYLPLSAPCRSVLMTAKALGIELNKKLLKLFEGGHLKPEFL-KI	46
Danio	-----MTGRQAVKAYLDLMSQPCRAVLIFLKHKNIPHTVEQIAIRKGEQKTPEFT-KL	52
Human	-----MGLELYLDLLSQPCRAVYIFAKKNIPFELRVDLIKQHLSDAFA-QV	48
Bos	-----MGLELYLDLLSQPCRAIYIFAKKNRIPFELRTVDLRKGQHLSDAFA-QV	48
Rattus	-----MGLELYLDLLSQPSRAVYIFAKKNIGIPQLRTVDLLKQHLSEQFS-QV	48

**Figure 2.14: Amino acid sequence alignment of Methylobacterium sp. DM4 and Methylophilus sp. DM11 dcmA with the other theta class GST.**

The alignment was conducted using Clustal Omega (<https://www.ebi.ac.uk/Tools/msa/clustalo/>). Amino acid sequences were obtained from UniProt database (<https://www.uniprot.org>) with the entry P21161 for *Methylobacterium* sp. DM4 dcmA, P43387 for *Methylophilus* sp. DM11 dcmA, P46433 for *Musca domestica* GSTT4, B0V1J9 for *Danio rerio* GSTT2, P30711 for Human GSTT1, Q2NL00 for *Bos taurus* GSTT1 and P30713 for *Rattus norvegicus* GSTT2.

#### 2.4.2.3 Zeta

Zeta class of cytosolic GST was initially discovered while studying the evolution of GST superfamily (Board et al., 1997). The unusual sequence of GST was observed within almost all species representative, including bacteria. TCHQ dehalogenase and isomerase have become the characteristic activities that presence within this class. The sequence RSXXXXRVRIAL is also become the motif within the N-terminal domain of prokaryote GST zeta class (Shehu et al., 2019).

A zeta-like GST in *Acidovorax* sp. KKS102, KKSG9, has been reported to share low amino acid sequence similarity with the other zeta GST. However, biochemical properties of this protein resemble the zeta class GST family. The functional studies of KKSG9 even indicating to a broader substrate specificity (Shehu & Alias, 2018).

Another bacteria zeta class GST (*NagL*) has also been identified in *Ralstonia* sp. U2 (Zhou et al., 2001). It has been confirmed that the enzyme exhibits maleyl pyruvate isomerase which involve in naphthalene metabolism (see **Figure 2.15**). Amino acid sequence of this GST was also found to follow the N-terminal motif of zeta class (Marsh et al., 2008).

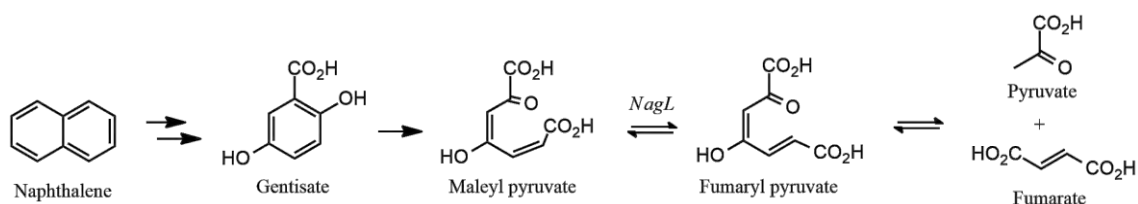


**Figure 2.15: Naphthalene metabolism**

#### 2.4.2.4 Chi

The first protein that became the prototype of this class is thermophilic cyanobacteria *Thermosynechococcus elongates* BP-1 and *Synechococcus elongates* PCC 6301 (Wikteliu & Stenberg, 2007). Identification of the amino acid sequence within the N-terminal domain showed that the GST proteins from those two microorganisms do not contain any cysteine residue. Those two GSTs also exhibit activity towards several basic substrates such as CDNB, 4-nitrobenzyl chloride, ethacrynic acid and 1,2-epoxy-3-(p-nitrophenoxy)propane at a moderate rate. However, high conjugation activity was observed towards several structurally different isothiocyanates. Another well-characterised chi class GST came from freshwater cyanobacteria *Synechocystis* PCC 6803 from gene sll0067 (Pandey, Singh, et al., 2015). Unlike the other bacterial GSTs, it was observed to react efficiently towards CDNB even when compared to mammalian enzymes. Moreover, this enzyme showed great stability over the pH 2 to 11. Pro53 was suspected to act as a hydrophobic staple and N-capping box, which is essential for stabilising the structure of this enzyme.

**Table 2.4: Comparison of bacterial cytosolic GST classes**

Class	Catalytic site	Activity towards CDNB	GSH-affinity column binding	Special Function	Distribution in bacteria
Beta	Cys	Low	Yes	Oxidoreductase	Proteobacteria, e.g.: <i>Pseudomonas</i> , <i>Enterobacter</i> , <i>Escherichia</i>
Theta	Ser	No	No	CDMC	Methylophilic bacteria, e.g.: <i>Methylobacterium</i> sp. DM4, <i>Methylophilus</i> sp. DM11
Zeta	Ser	?	?	TCHQ dehalogenase, isomerase	<i>Ralstonia</i> sp. U2, <i>Pseudomonas aeruginosa</i> ATCC 15692
Chi	?	High	?	Conjugation towards isothiocyanates	Cyanobacteria and gram-positive bacteria, e.g.: <i>Thermosynechococcus elongates</i> BP-1
Eta	Arg	Moderate	No	Peroxidase	<i>Agrobacterium tumefaciens</i>
Rho	?	Moderate	?	Conjugation towards dichloroacetate	<i>Synechosystis</i> PCC 6803
Nu	Thr (High affinity towards GSSG; can bind with two GSH simultaneously)	Low	?	Disulfide-bond oxidoreductase, organic hydro- peroxidase	<i>E. coli</i> , <i>Novosphingobium aromaticivorans</i> , <i>Sphingobium</i> sp. SYK-6
Xi	Cys	No	?	Glutathionyl-hydroquinone reductase	<i>Sphingobium chlorophenolicum</i> , <i>E. coli</i>

#### 2.4.2.5 Eta

The pathogenic soil microorganism *Agrobacterium tumefaciens* C58 GST (*AtuGSTH1-1*) is the prototype of GST eta class. The finding of this class began when the catalytical and structural studies of this enzyme was conducted. Amino acid sequence analysis of *AtuGSTH1-1* shown that this enzyme shares low similarity with other class of cytosolic GST. The high conjugation activity towards aryl halides and significant peroxidase activity of organic hydroperoxides was observed. The crystal structure of *AtuGSTH1-1* has been obtained in the complex with S-(p-nitrobenzyl)-glutathione. Although *AtuGSTH1-1* possesses distinct characteristic in amino acid sequence and activity, it still follows the general canonical GST fold (Skopelitou et al., 2012). The lack of classic catalytic residues, such as serine, cysteine and tyrosine, has become the identity of this class. Site-directed mutagenesis revealed that the residue of arginine (Arg34) is essential for the catalytic mechanism. Phe22, Ser25 and Arg187 are also reported to be responsible to promote the efficiency and specificity of the enzyme.

#### 2.4.2.6 Rho

Rho class of cytosolic GST was initially reported from cyanobacterium *Synechosystis* PCC 6803 (sll1545). Sll1545 shows the strong GSH-dependent peroxidase activity, which is one of the characteristics of alpha and theta class. However, the similarity between sll1545 and those two cytosolic GST classes is only around 20%. This protein also exhibits the high conjugation activity towards dichloroacetate which has not been observed in other bacterial GST. In silico structural studies of this protein found that it has a differ pattern with other class of GST (Pandey, Chhetri, et al., 2015).

#### 2.4.2.7 Nu

Nu class of GST was first identified within two homologous proteins of *Escherichia coli* K12, YfcG and YghU. These proteins were classified into different class of GST due to its distinct activity and structure. Unlike the other GSTs, YfcG and YghU did not show any conjugation activity towards electrophilic substrates. However, an efficient reductase activity of disulphide-bonds was observed towards 2-hydroxyethyl disulfide. In addition, functional studies of YghU also shown that this protein promotes the reduction of several hydroxyperoxide.

The reduction towards 2-hydroxyethyl disulphide which catalyse by YfcG is considered as a unique feature due to the lack of cysteine residue in YfcG active site which then suggest that the reaction occurs without covalent bond involvement of sulfhydryl group. The other unusual thing was the oxidised form of glutathione (GSSG) was revealed to bind in the active site of this protein, instead of GSH, even though the crystal was obtained under the presence of GSH (Wadington et al., 2009).

The anomaly was also observed within YghU. Based on structural studies and equilibrium binding data, it was known that YghU binds with two molecules of GSH in its active site. The superposition between YfcG in complex with GSSG and YghU in complex with two molecules of GSH showed that these two proteins have similar structure, including the orientation of both GSSG and two GSH molecule. It then lead to the suggestion that those two proteins are the oxidised and reduced form of GSH-dependent disulphide-bond oxidoreductases (Stourman et al., 2011).

#### 2.4.2.8 Xi

Within bacteria, GST xi class can be found in both gram-negative and gram-positive. This class is specifically known with its glutathionyl-hydroquinone reductase (GS-HQR)

activity (see 2.3.1.1). The prototype GST of this class was first identified within *Phanerochaete chrysosporium* (PcGSTX1), the white rot fungus which is known to have the ability to degrade lignin. PcGSTX1 was initially classified into omega class (subclass I) due to its sequence similarity, including its conserved cysteine residue. But then, the 3D structure of PcGSTX1 has found to possess the unique features 1) a long N-terminal coil containing 77 residues 2) a loop that link  $\beta 2$  and  $\alpha 2$  was extended by 20 residues 3) a C-terminal extension which create the ninth  $\alpha$ -helix followed by extra 20 residues (Meux et al., 2011). Those unique features forming the unusual dimerization mode. The binding pocket within the G-site was also seemed to be buried deeper than other typical GSTs.

PcpF from *Sphingobium chlorophenolicum* (ScPcpF) and YqjG from *E. coli* (EcYqjG) are the examples of microbial xi class GST which have been well studied. Both ScPcpF and EcYqjG possess the same unique features as PcGSTX1, including the conserved residues and atypical dimerization mode. The crystal structure of complex EcYqjG with GSH and GS-menadione were successfully obtained, exhibiting the large H-site which allows big substituted hydroquinones to bind as a substrate (Green et al., 2012).

## 2.5 KKSG6

KKSG6 (NCBI Reference Sequence: WP\_015014999.1) is one of eleven putative GSTs within *Acidovorax* sp. KKS102, a proteobacteria which is known to have degradation activity towards biphenyl/polychlorinated biphenyl. KKSG6 consists of 202 amino acids and is predicted to have an isoelectric point and molecular weight at pH 6.37 and 22.14 kDa (Gasteiger et al., 2005). KKSG6 belongs to the beta class of cytosolic GST subfamily which proven by high sequence identity with the other member of beta class (see **Table 2.5**) and conserve cysteine residue within the GSH site (see **Figure 2.16**).

**Table 2.5: Identity percentage of KKSG6 with the other member of beta class GST**

Member of Beta Class	UniProt Accession Number	% Identity with KKSG6
<i>Burkholderia xenovorans</i> GST (BphK)	Q59721	48.02
<i>Proteus mirabilis</i> GST (PmGST)	P15214	45.05
<i>Escherichia coli</i> GST (EcGST)	P0A9D2	42.79
<i>Ochrobactrum anthropic</i> GST (OaGST)	P81065	39.60

The sequence of each member of beta class was obtain from UniProt database (<https://www.uniprot.org/>). The identity percentage was determined using NCBI blastp ([https://blast.ncbi.nlm.nih.gov/Blast.cgi?PROGRAM=blastp&PAGE\\_TYPE=BlastSearch&BLAST\\_SPEC=blast2seq&LINK\\_LOC=blasttab](https://blast.ncbi.nlm.nih.gov/Blast.cgi?PROGRAM=blastp&PAGE_TYPE=BlastSearch&BLAST_SPEC=blast2seq&LINK_LOC=blasttab)) with default parameter.

```

OaGST      MKLYYKVGACSLAPHIILSEAGLPYELEAVDLKAKKTADGGDYFAVNPRGAVPALEVKPG 60
KKSG6      MKLYYAPGACSLAVHIALREVGVAFDLVKVDLVRHTTETGANYLDISPRGYVPLLELADQ 60
bphK       MKLYYSPGACSLSPHIALREAGLNFEVLVQVDLASKKTASGQDYLEINPAGYVPCQLDDG 60
PmGST      MKLYYTPGSCSLSPHIVLRETGLDFSIERIDLRKKTESGKDFLAINPKGQVPVLQLDNG 60
EcGST      MKLFYKPGACSLASHITLRESGKDFTLVSVDLMKKRLENGDDYFAVNPKGQVPALLLDDG 60

```

**Figure 2.16: Amino acids alignment of KKSG6 and other members of beta class GST.**

The alignment was performed using Clustal Omega (<https://www.ebi.ac.uk/Tools/msa/clustalo/>) with default parameter. Amino acid sequences were obtained from UniProt database (<https://www.uniprot.org/>) with the same accession number listed in Table 2.5.

## CHAPTER 3: METHODOLOGY

### 3.1 Materials

Herewith are listed the materials used in this research including chemicals, solutions, consumables and instruments. The *E. coli* strain and expression vector which also used to express the protein are also briefly explained.

#### 3.1.1 Chemicals

The chemicals used in this research are LB Broth (Friendemann Schmidt), Difco™ LB Agar (Becton Dickinson), Ampicillin Sodium Salt (Nalacai Tesque), Kanamycin Sulfate (Calbiochem), Streptomycin (Gibco), Gentamicin (Gibco), Tetracycline Hydrochloride (Duchefa Biochemie), Chloramphenicol (Duchefa Biochemie), Accura™ High-Fidelity Polymerase (Lucigen), Agarose LE (Promega), PrepEase® MiniSpin Plasmid Kit (USB from Affymetrix), *SacI* (NEB), SYBR® Green (Invitrogen), L-Glutathione reduced (Sigma-Aldrich), CelLytic™ B (Sigma), IPTG, 30% Acrylamide/Bis Solution 37.5:1 (Bio-Rad), SDS (Promega), APS, TEMED (Bio-Rad), 1-Butanol (Sigma-Aldrich), Methanol (System), Ethanol (System), Glacial Acetic Acid (Merck), EDTA (Sigma), Stacking Gel Buffer for PAGE (Bio-Rad), Resolving Gel Buffer for PAGE (Bio-Rad), DTT (Bio-Rad), Bromophenol Blue (Sigma-Aldrich), Glycerol (Friendemann Schmidt), Brilliant Blue R (Sigma-Aldrich) and distilled water.

#### 3.1.2 Solutions

All solutions used in this research and their composition are listed in **Table 3.1**.

**Table 3.1: Solutions and their compositions**

Solutions	Composition
1× TAE buffer	40mM Tris, 20mM Glacial acetic acid and 1mM EDTA
1× SDS-PAGE running buffer	25 mM Tris, 192 mM Glycine and 0.1% (w/v) SDS
4× SDS-PAGE sample buffer	200 mM Tris-Cl (pH 6.8), 400 mM DTT, 8% (w/v) SDS, 0.4% (w/v) bromophenol blue and 40% (v/v) glycerol
SDS-PAGE staining solution	0.25% (w/v) Coomassie Blue R-250, 50% (v/v) Methanol and 10% (v/v) Glacial acetic acid
SDS-PAGE destaining solution	30% (v/v) Methanol and 10% (v/v) Glacial acetic acid

### 3.1.3 Instruments

Here are the instruments used in this research: autoclave, incubator, shaking incubator, vortex, spectrophotometer, water bath, tabletop centrifuge, thermal cyclers (Bio-Rad), horizontal electrophoresis system (Bio-Rad), Äkta Purifier (GE Healthcare) and Mini-PROTEAN® Tetra Vertical Electrophoresis Cell (Bio-Rad).

### 3.1.4 *Escherichia coli* BL21 Star™ (DE3)

*Escherichia coli* BL21 Star™ (DE3) is a commercial gram-negative bacterial strain which used as a protein expression host. This strain contains  $\lambda$  DE3 lysogen that carries the T7 RNA polymerase gene under the *lacUV5* promoter. RNase E in this strain has been mutated to devoid the degradation ability towards mRNA, resulting the increase of mRNA stability. It is also designed to reduce the heterologous protein degradation within the cell by abolishing the *lon* protease and outer membrane OmpT protease. In general, the yield of recombinant protein from T7-based expression vectors will increase within this strain.

### 3.1.5 pET101/D-TOPO®-KKSG6

pET101/D-TOPO®-KKSG6 is a commercial expression vector harbouring KKSG6 gene. The expression of KKSG6 within this plasmid is regulated with T7 promoter. For selection purpose, pET101/D-TOPO®-KKSG6 is designed with ampicillin resistance marker. The genetic map of this plasmid can be seen in **Figure 3.1**.

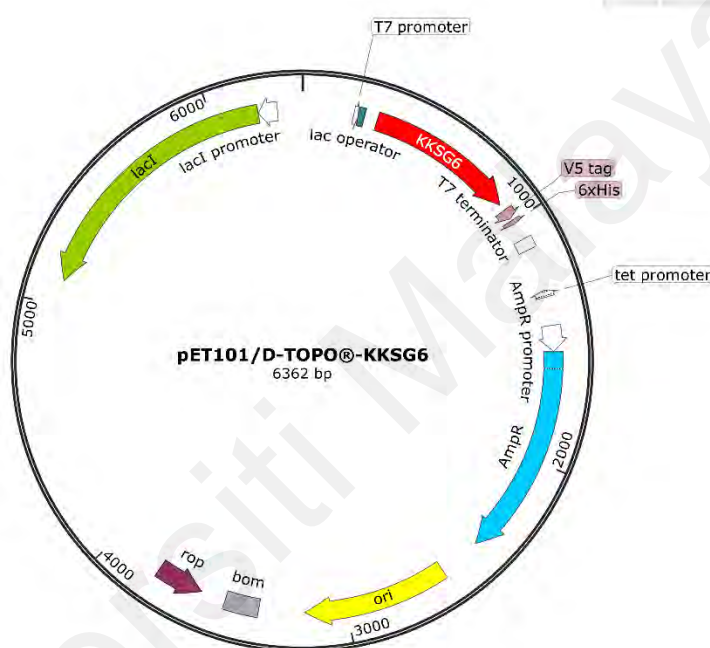


**Figure 3.1: pET101/D-TOPO®-KKSG6**

## 3.2 Methods

The workflow in this research is provided in **Figure 3.2**. All methods used in this research from bacterial retrieval to protein functional studies are further explained from section 3.2.1 to 3.2.12.

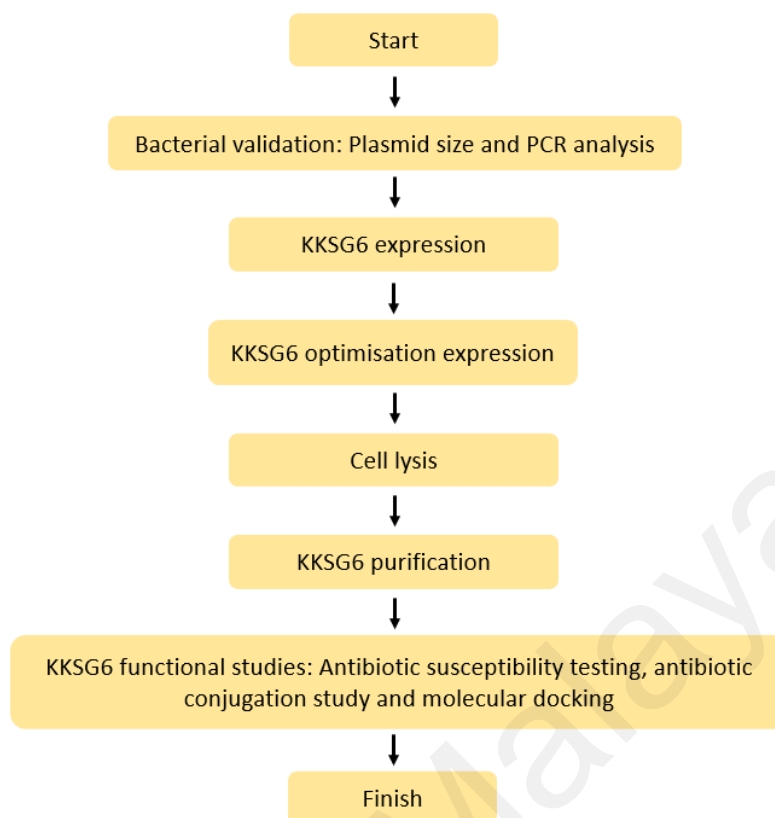


**Figure 3.2: Research workflow**

### 3.2.1 Bacteria retrieval

*Escherichia coli* BL21 Star™ (DE3) harbouring pET101/D-TOPO®-KKS6 was retrieved from glycerol stock by several steps. First, the frozen stock was thawed in room temperature for about 30 minutes. The stock was then mixed by inverting the tubes several times. 50  $\mu$ L of the stock solution was then spread into LB plate containing 100  $\mu$ g/mL ampicillin. The plate was then incubated in 37°C for 16-18 hours.

### 3.2.2 Bacterial validation

To validate whether the bacteria which has been retrieved previously was the one carrying the pET101/D-TOPO®-KKS6, plasmid size analysis and polymerase chain

reaction was carried out. All steps involved in validating the bacteria are explained further in 3.2.2.1 and 3.2.2.2.

#### **3.2.2.1 Plasmid size analysis**

In general, plasmid size analysis was conducted by confirming whether the plasmid which extracted from the bacteria has the same size with the intended one. To do so, the plasmid needed to be extracted first from the cells. Then, the pure plasmid was linearised using restriction enzyme. Last, the linear plasmid was electrophoresised in agarose gel matrix to confirm its size.

##### **3.2.2.1.1 Plasmid extraction**

The very first thing that needs to be prepared for plasmid size analysis is the pure pET101/D-TOPO<sup>®</sup>-KKSG6. It can be obtained by the process called plasmid extraction. In this research, plasmid extraction was performed using PrepEase<sup>®</sup> MiniSpin Plasmid Kit (USB from Affymetrix). The plasmid acquired from this process was then stored in -20°C fridge for further analysis.

##### **3.2.2.1.2 Plasmid linearisation**

Before the plasmid size analysis performed, the pure pET101/D-TOPO<sup>®</sup>-KKSG6 obtained from extraction process needs to be linearised first. The plasmid was cut using *SacI* (NEB) by incubating the reaction mixture in **Table 3.2** for 1 hour in 37°C. The mixture was then immediately electrophoresised in 1% agarose gel (method as in 3.2.3).

**Table 3.2: Linearisation reaction mixture**

Components	Volume (μL)
pET101/D-TOPO®-KKSG6	2
CutSmart® Buffer	0.5
Nuclease-free H <sub>2</sub> O	2.2
<i>Sac</i> I	0.3
Total volume	5

### 3.2.2.2 Polymerase chain reaction

The polymerase chain reaction (PCR) which carried out in this study was performed using Accura™ High-Fidelity Polymerase (Lucigen). The reaction mixture was made by mixing some components as listed in **Table 3.3**. The PCR was then set on the thermal cyclers (Bio-Rad) under the condition summarised in **Figure 3.3**. Once the process completed, the DNA mixture was then immediately electrophoresised in 1% agarose gel matrix.

**Table 3.3: Polymerase chain reaction recipe**

Component	Volume (μL)
10× GC Buffer	5
5 M Betaine	20
25 mM dNTPs	8
10 μM Forward primer	2
10 μM Reverse primer	2
2 U/μL Accura High-Fidelity Polymerase	0.5
Nuclease-free H <sub>2</sub> O	12.5
Total volume	50

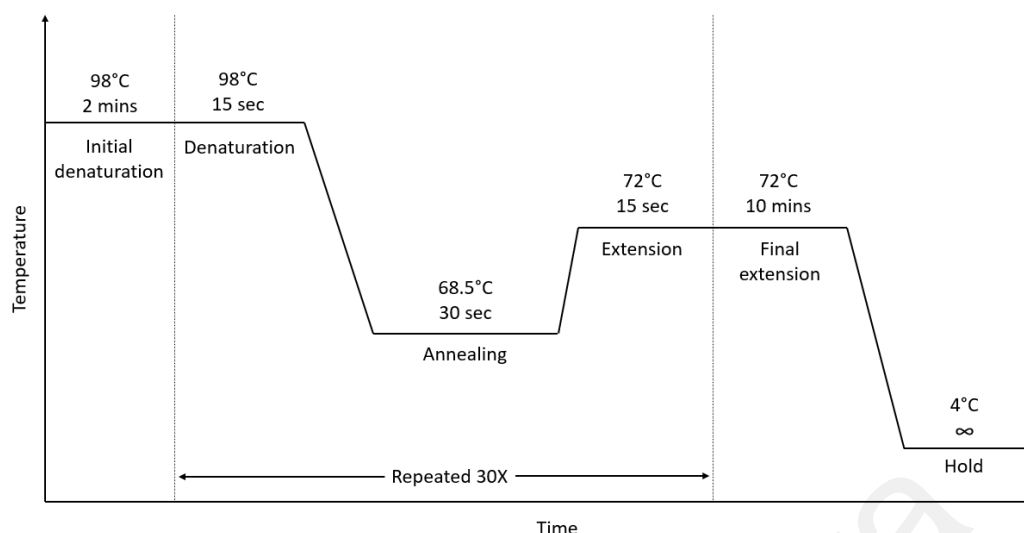


**Figure 3.3: Polymerase chain reaction condition**

### 3.2.3 Agarose electrophoresis

The DNA electrophoresis was carried out using horizontal electrophoresis system (Bio-Rad) by applying 80V electrical current to the 1% agarose gel for 35 minutes. To stain the gel and load the DNA sample, SYBR<sup>®</sup> Green (Invitrogen) and 6× Loading Dye (NEB) was utilised.

### 3.2.4 Expression of KKSG6

To express the KKSG6 gene, the overnight culture needs to be prepared by inoculating the *E. coli* BL21 Star<sup>™</sup> (DE3) harbouring pET101/D-TOPO<sup>®</sup>-KKSG6 into the 5 mL LB medium which contain 100 µg/mL ampicillin. The culture was then placed into the 37°C shaking incubator for 12-16 hours. 1% of overnight culture was then transferred into the new LB media containing 100 µg/mL ampicillin. After that, the culture was shaken with angular velocity 150 rpm in 37°C until the OD in 600 nm reach 0.6. The IPTG was then added to a final concentration 0.5 mM. The culture was then re-shaken for another 4

hours. To harvest the cells, the culture was centrifuged with angular velocity  $5000\times g$  for 15 minutes. The cell pellet was then stored in  $-20^{\circ}\text{C}$  fridge for further experiments.

### **3.2.5 Optimisation expression of KKSG6**

The optimisation of KKSG6 expression was performed by comparing the total activity of crude extract under the variation of post-induction incubation time and IPTG concentration. The expression was carried out following the procedure explained in 3.2.4. Total activity was then determined as stated in 3.2.9.

#### **3.2.5.1 Post-induction incubation time optimisation**

The effect of post-induction incubation time on KKSG6 production was evaluated by comparing the total activity of each culture from different time variations. Once the culture reached its exponential phase ( $\text{OD}_{600} \sim 0.8$ ), 0.5 mM IPTG was added to induce the KKSG6 expression. After that, the culture was re-incubated in  $37^{\circ}\text{C}$  shaking incubator. 1.5 mL of culture was then being sampled after 4, 5, 6 and 24 hours incubation, followed by the observation of  $\text{OD}_{600}$ . The bacterial cell was harvested and lysed in accordance with the procedure described in 3.2.4 and 3.2.6. The total activity of crude extract was then determined as stated in 3.2.9.

#### **3.2.5.2 IPTG concentration optimisation**

The effect of IPTG concentration on KKSG6 expression was evaluated by comparing the total activity of each culture from different concentration variations. Once the culture reached its exponential phase ( $\text{OD}_{600} \sim 0.8$ ), 1, 0.5, 0.25 and 0.1 mM IPTG was added to induce the KKSG6 expression. After that, the culture was re-incubated in  $37^{\circ}\text{C}$  shaking incubator for 5 hours. 1.5 mL of each culture was then being sampled, followed by the

observation of OD<sub>600</sub>. The bacterial cell was harvested and lysed in accordance with the procedure described in 3.2.4 and 3.2.6. The total activity of crude extract was then determined as stated in 3.2.9.

### 3.2.6 Bacteria cell lysis

In this research, chemical lysis was performed to break the bacteria membrane cell. First, 20 mL of CelLytic™ B (Sigma) was added to each grams the frozen cell pellet which obtained from the previous expression process. The cell pellet was then resuspended by pipetting. After that, the culture was shaken in room temperature for 15 minutes. Then, it was centrifuged for 15 minutes in 4°C with angular velocity 12,000×g. The lysate (crude extract) was then stored in -20°C fridge for further experiments.

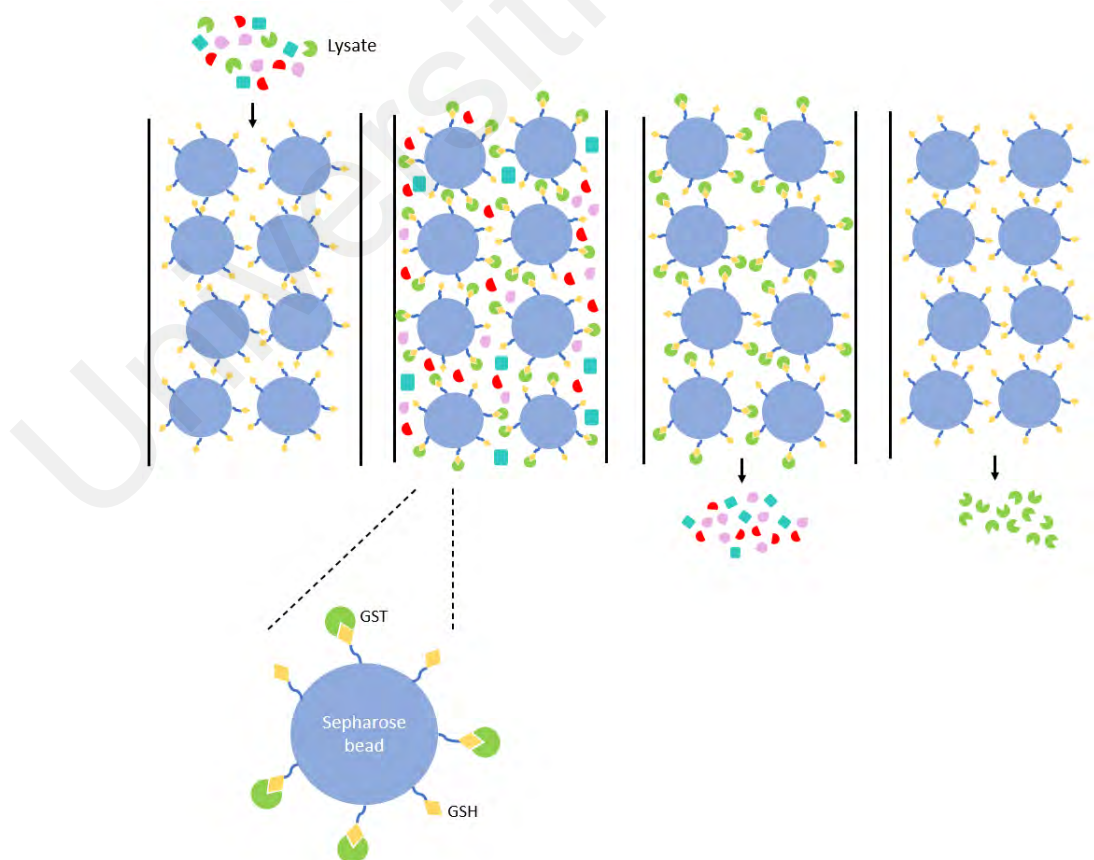


**Figure 3.4: GSTrap™ HP column principles**

### 3.2.7 Protein purification

The protein purification was carried out using Äkta Purifier (GE Healthcare) with GStap™ HP column (see **Figure 3.4** for the principles). The column was initially equilibrated with 25 mM phosphate buffer pH 7.4 with the flow rate 0.3 mL/minute. Once the column equilibration done, 5 mL of sample was then injected. After the UV line drop to the base, indicating there was no protein detected, the GST was eluted with 10 mM GSH solution in 25 mM phosphate buffer pH 7.4. The elution fraction was then collected and stored in -20°C fridge for further experiments.

### 3.2.8 Sodium dodecyl sulfate-polyacrilamide gel electrophoresis

Sodium dodecyl sulfate-polyacrilamide gel electrophoresis (SDS-PAGE) is a common method to analyse the proteins based on its mobility under the electric current. Polyacrilamide gel was prepared by mixing the components listed in **Table 3.4**. The electrophoresis was performed using Mini-PROTEAN® Tetra Vertical Electrophoresis Cell (Bio-Rad) by applying 110V electrical current for 90 minutes.

**Table 3.4: Polyacrilamide gel components**

Components	Volume (μL)	
	Separating	Stacking
ddH <sub>2</sub> O	1600	1370
1.5 M Tris-HCl pH 8.8	1300	-
0.5 M tris-HCl pH 6.8	-	250
10% SDS	50	20
30% Acrylamide	2000	340
10% APS	50	20
TEMED	5	3

### 3.2.9 Glutathione S-transferase assay

The GST activity was examined following the steps explained by Habig et al., (1974) using CDNB as a substrate. The absorbance of reaction mixture (see **Table 3.5**) was observed for 10 minutes at  $\lambda_{340\text{nm}}$ , starting from the addition of CDNB. Molar extinction coefficient ( $\epsilon$ ) is  $0.0096 \mu\text{M}^{-1} \text{cm}^{-1}$ .

**Table 3.5: Glutathione S-transferase assay mixture**

Components	Volume ( $\mu\text{L}$ )
0.1 M Phosphate buffer pH 6.6	2850
60 mM Glutathione	50
60 mM CDNB	50
Enzyme	50
Total	3000

### 3.2.10 Antibiotic susceptibility testing

Antibiotic susceptibility testing was conducted using standard broth dilution (Jorgensen & Ferraro, 2009). The growth of *E. coli* BL21 Star™ (DE3) containing pET101/D-TOPO®-KKSG6 which previously induced with 0.1 mM IPTG was observed under various antibiotics. As a control, the growth of un-induced culture was also observed. Five antibiotics in total were tested: kanamycin, streptomycin, gentamycin, tetracycline and chloramphenicol. Two times serial dilution for each antibiotic used in this research are summarised in **Table 3.6**. The significant difference of inhibition growth percentage between bacterial cells with and without KKSG6 was statistically evaluated by paired T-test.

**Table 3.6: Antibiotics concentrations for serial dilution**

Antibiotics	Concentrations ( $\mu\text{g/mL}$ )				
Kanamycin	50	25	12.5	6.25	3.125
Streptomycin	50	25	12.5	6.25	3.125
Gentamicin	10	5	2.5	1.25	0.625
Tetracycline	10	5	2.5	1.25	0.625
Chloramphenicol	5	2.5	1.25	0.625	0.3125

### 3.2.11 Antibiotic conjugation study

KKSG6 conjugation activity towards antibiotics was performed by confirming the presence of GSH-antibiotic conjugates as the enzymatic reaction product through thin layer chromatography (TLC). The enzymatic reaction between GSH and antibiotics was conducted by mixing the components in **Table 3.5**, where CDNB was replaced by kanamycin, tetracycline and chloramphenicol. After 10 minutes, the small amount of reaction mixture was transferred to silica gel. The TLC was then developed for 2 hours after the chamber had been previously saturated with 1-butanol: acetic acid: distilled water (12:3:5). The glutathione-conjugates were visualised with 0.25% (w/v) ninhydrin in acetone (Rogers et al., 1999). The GST conjugation assay towards antibiotics was also carried out in accordance with procedures given in 3.2.9.

### 3.2.12 Molecular docking

Interaction between KKSG6 and antibiotics were modelled by conducting molecular docking. All details involved in docking process are further explained in the subsections below.

### 3.2.12.1 Structure prediction

KKSG6 structure was predicted using comparative modelling in SWISS-MODEL server (Bertoni et al., 2017). Glutathione S-transferase from *Yersinia pestis* (PDB ID: 4GCI) with 49.75% identity and 1.5 Å resolution was selected as a template. The KKSG6 modelled structure was then refined using DeepRefiner (Shuvo et al., 2021). MolProbity was used to validate the atom contacts and geometry of the modelled structure (Williams et al., 2018).

### 3.2.12.2 Ligand structure preparation

All antibiotics structures in SDF file format were obtained from PubChem (<https://pubchem.ncbi.nlm.nih.gov/>). The file format was then converted to PDBQT using Open Babel GUI (version 2.3.1).

### 3.2.12.3 Protein-ligand docking

Molecular docking was carried out using AutoDock (version 4.2.6) (Morris et al., 2009). Its graphical user interface AutoDockTools (version 1.5.6) was used to add the enzyme partial charge and polar hydrogen. The same programme was also used to set the ligands' root, number of torsion and partial charge. The docking region was defined using AutoGrid (version 4.2.6). For docking within dimer interface, the grid was set to cover the area with dimension of 20, 30, 20 Å from -18.316, 94.732, 59.716 midpoint. Meanwhile for H-site docking, the grid was set in the midpoint of -16.3, 88.4, 70.5 and dimension of 13.5, 11.3, 11.3 Å. A genetic algorithm with default parameters was used to perform the docking process, except for the number of runs and population size which were set to be 50 and 300 respectively. Once docking process finished, the interaction

between protein and ligand was profiled using PLIP (Adasme et al., 2021; Salentin et al., 2015).

Universiti Malaya

## CHAPTER 4: RESULT

### 4.1 Bacterial retrieval

*E. coli* BL21 Star™ (DE3) harbouring pET101/D-TOPO®-KKSG6 has been retrieved with the procedure explained in 3.2.1. The plate of the bacteria can be seen in **Figure 4.1**.

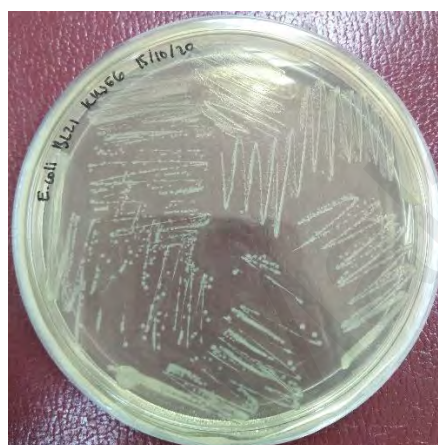


**Figure 4.1: Bacterial plate**

The white stripes on the plate indicated bacterial colonies of *E. coli* BL21 Star™ (DE3) harbouring pET101/D-TOPO®-KKSG6.

### 4.2 Bacterial validation

In this research, bacterial validation was carried out by doing plasmid size and PCR analysis. Results of the validation process can be seen in 4.2.1 and 4.2.2.

#### 4.2.1 Plasmid size analysis

The pET101/D-TOPO®-KKSG6 extraction was carried out following the procedure explained in 3.2.2.1.1 to obtain the pure plasmid. The success of extraction process was then confirmed by electrophoresising the plasmid in agarose gel matrix. The electrophoregram of plasmid extraction is shown in **Figure 4.2**. Once the pure plasmid

was obtained, it was linearised using the method explained in 3.2.2.1.2. The size analysis was then carried out by observing the migration pattern of linearised plasmid under the agarose gel matrix. The electrophoregram of plasmid size analysis can be seen in **Figure 4.3**.

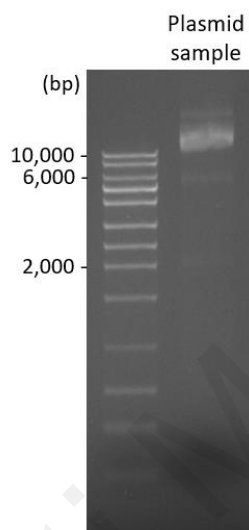


**Figure 4.2: pET101/D-TOPO®-KKSG6 extraction electrophoregram**

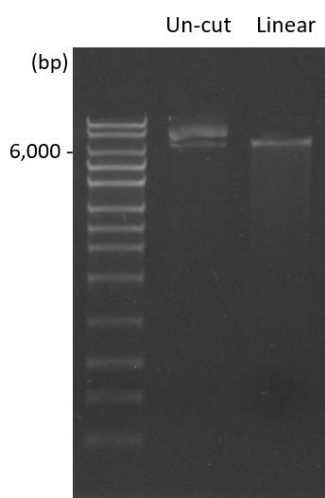


**Figure 4.3: pET101/D-TOPO®-KKSG6 size analysis electrophoregram**

#### 4.2.2 PCR analysis

PCR analysis was conducted following the method described in section 3.2.2.2. The electrophoregram of PCR analysis performed in this research is presented in **Figure 4.4**.

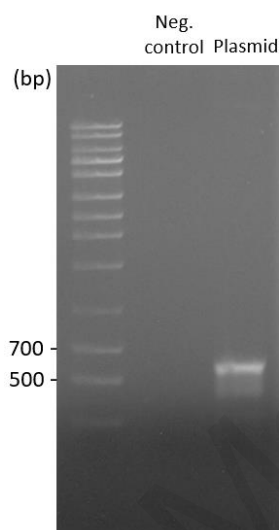


**Figure 4.4: PCR colony electrophoregram**

#### 4.3 Expression of KKSG6

The expression of KKSG6 was carried out following the steps as explained in 3.2.4. To confirm the success of expression process, the total protein was electrophoresised through polyacrylamide matrix following the procedure explained in 3.2.8. The electrophoregram of KKSG6 expression is provided in **Figure 4.5**.

#### 4.4 Optimisation expression of KKSG6

The optimisation of KKSG6 production was carried out in accordance with the procedure stated in 3.2.5. **Figure 4.6** and **Figure 4.7** are respectively summarised the effect of post-induction incubation time and IPTG concentration on the KKSG6 expression (see Appendix B for raw data).

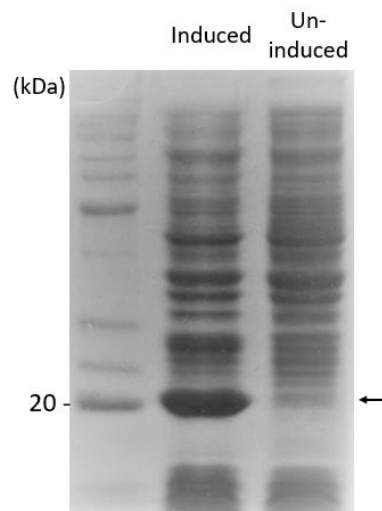


**Figure 4.5: KKSG6 expression electrophoregram**

The arrow indicates the protein band intensity difference between induced and un-induced bacterial cells at 20 kDa.

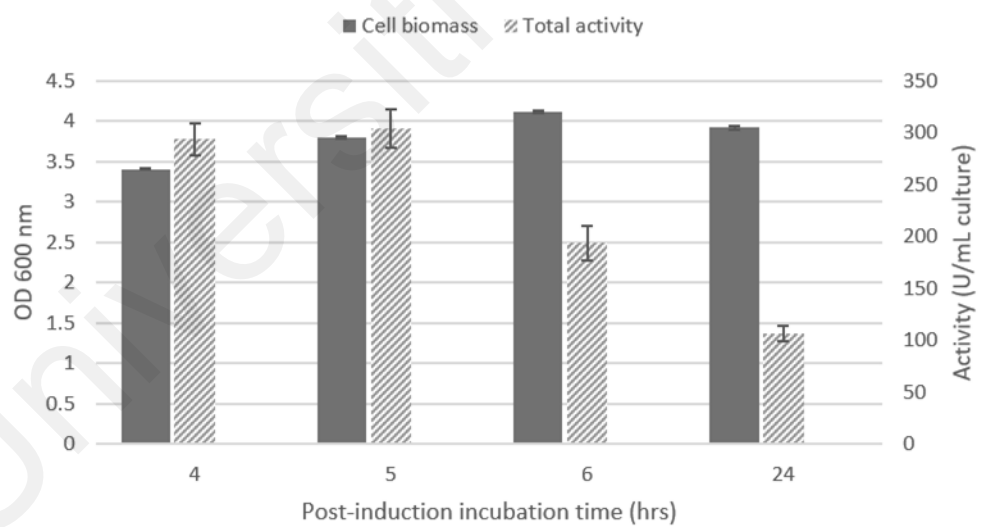


**Figure 4.6: Effect of post-induction incubation time on KKSG6 expression**

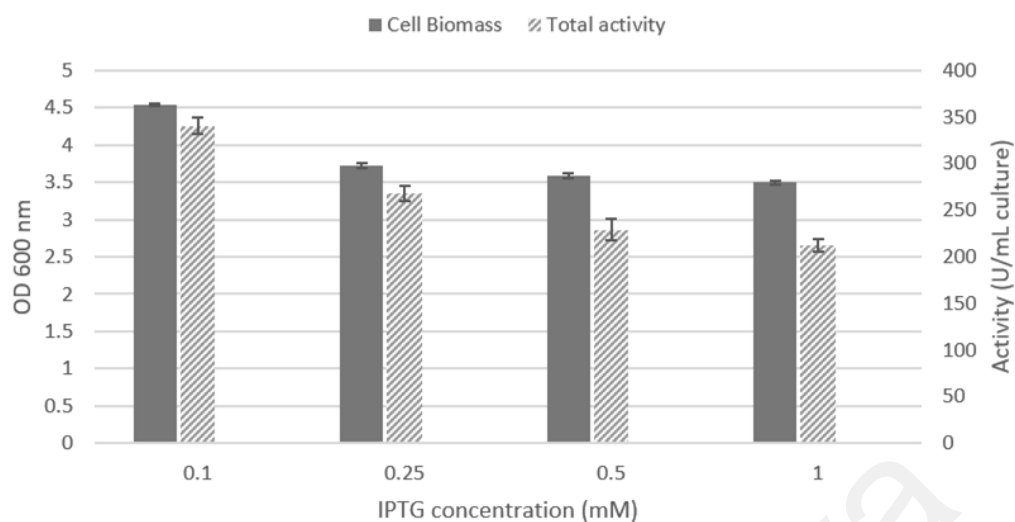


**Figure 4.7: Effect of IPTG concentration on KKSG6 expression**

#### 4.5 Bacterial cell lysis

In this research, the cell lysis was carried out chemically using CelLytic™ B (Sigma) as explained in 3.2.6. To verify the success of lysis process, both cell pellet and lysate fraction obtained from the centrifugation was electrophoresed. The electrophoregram of cell lysis can be seen in **Figure 4.8**.

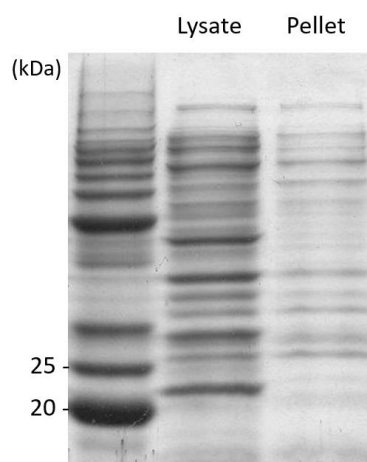


**Figure 4.8: Cell lysis electrophoregram**

#### 4.6 Protein purification

The protein purification was carried out following the procedure in 3.2.7. The success of this process was confirmed by electrophoresing the eluted fraction. The electrophoregram of protein purification is shown in **Figure 4.9**.

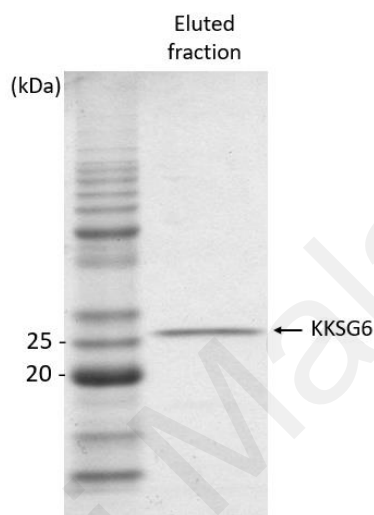


**Figure 4.9: Protein purification electrophoregram**

The purified KKSG6 migrated at approximately 25 kDa, as indicated by arrow. The gel was stained with 0.25% (w/v) Coomassie Blue R-250 in 50% (v/v) Methanol and 10% (v/v) Glacial acetic acid.

#### 4.7 Antibiotic susceptibility testing

The antibiotic susceptibility testing was conducted as explained in 3.2.10. The graph of bacterial growth under several concentrations of antibiotics is given in **Figure 4.10-14** (see Appendix C for raw data).

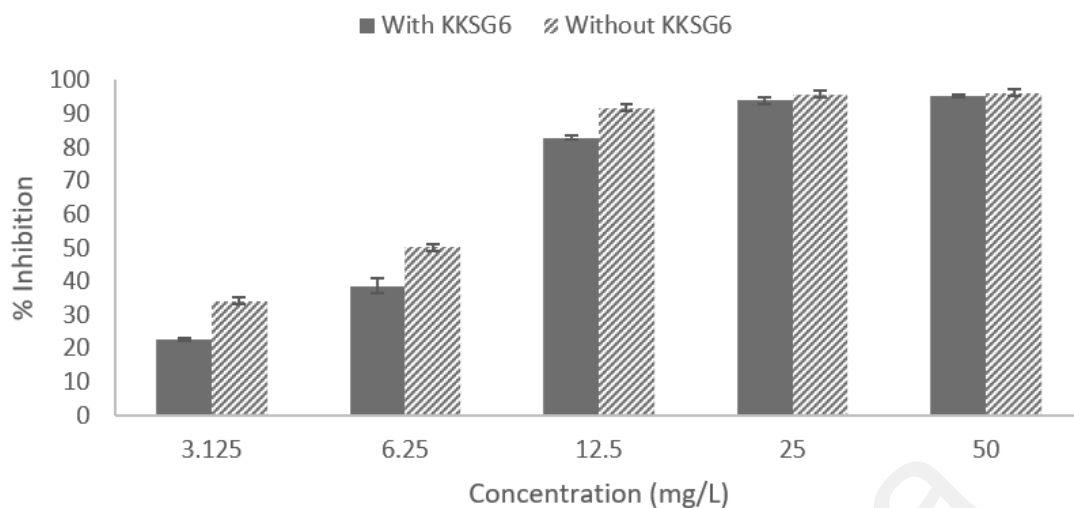


**Figure 4.10: *E. coli* susceptibility towards kanamycin**

The graph indicates the susceptibility of *E. coli* towards kanamycin in the presence and absence of KKSG6 gene.

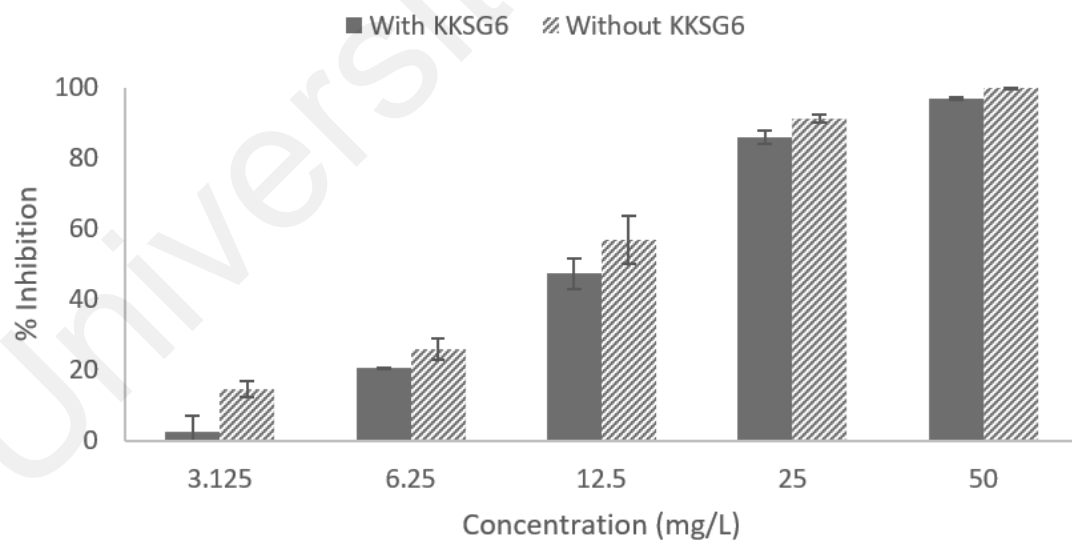


**Figure 4.11: *E. coli* susceptibility towards streptomycin**

The graph indicates the susceptibility of *E. coli* towards streptomycin in the presence and absence of KKSG6 gene.

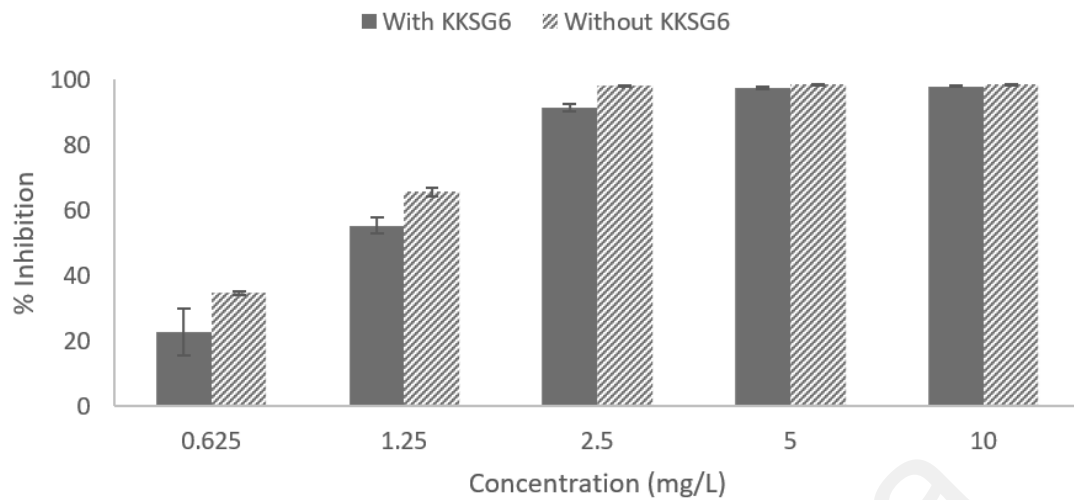


**Figure 4.12: *E. coli* susceptibility towards gentamycin**

The graph indicates the susceptibility of *E. coli* towards gentamycin in the presence and absence of KKSG6 gene.

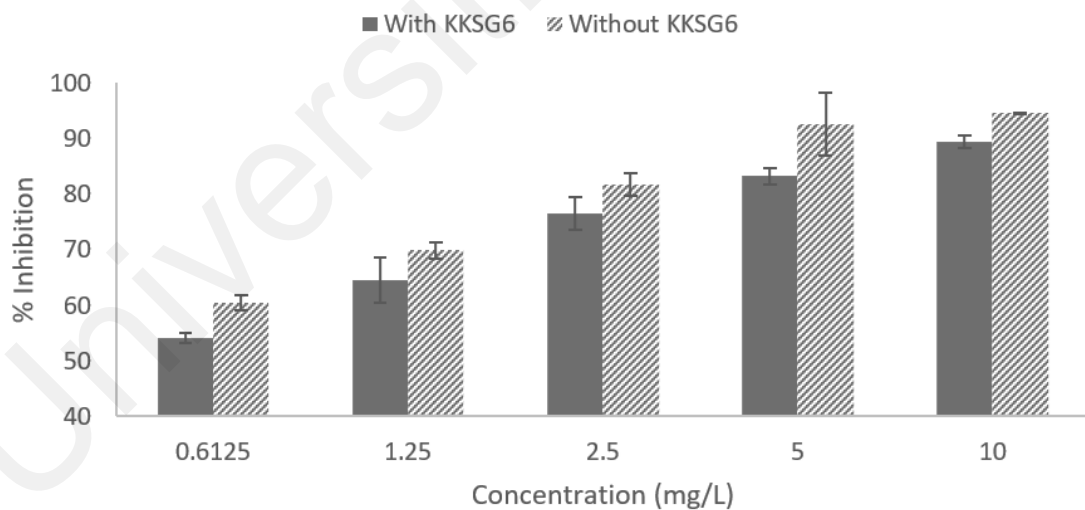


**Figure 4.13: *E. coli* susceptibility towards tetracycline**

The graph indicates the susceptibility of *E. coli* towards tetracycline in the presence and absence of KKSG6 gene.

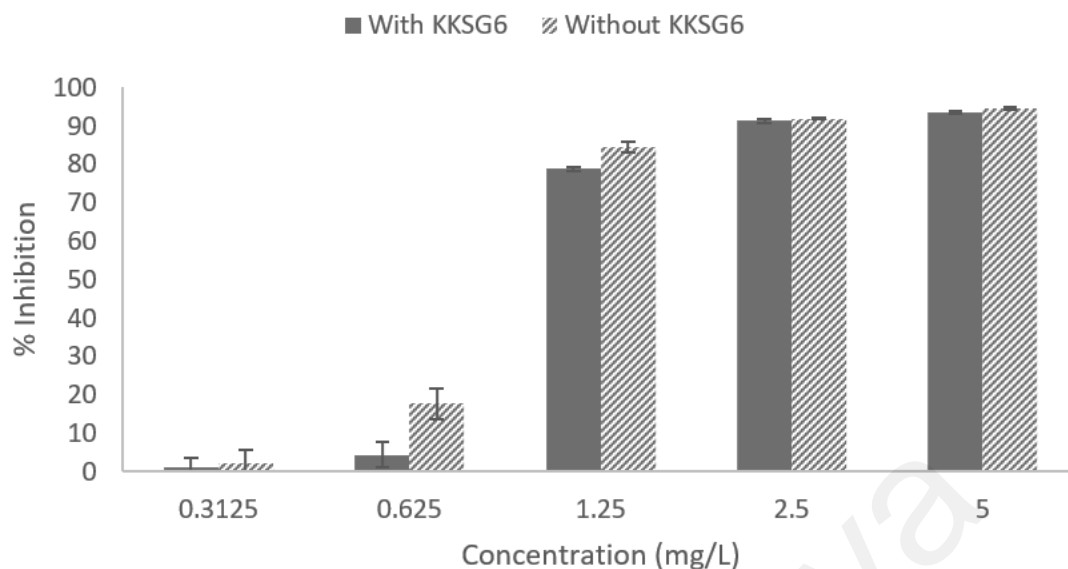


**Figure 4.14: *E. coli* susceptibility towards chloramphenicol**

The graph indicates the susceptibility of *E. coli* towards chloramphenicol in the presence and absence of KKSG6 gene.

#### 4.8 Antibiotic conjugation study

The antibiotic conjugation study towards kanamycin, tetracycline and chloramphenicol was performed following the methods stated in 3.2.11. Thin layer chromatogram of antibiotic conjugate is provided in **Figure 4.15**. There was no conjugation occurring between GSH and kanamycin or tetracycline observed (data not shown). The KKSG6 assay with and without the presence of chloramphenicol is summarised in **Figure 4.16**.



**Figure 4.15: Thin layer chromatogram of antibiotic conjugate**

The circled region shows the conjugated products. Lane 1: GSH + CDNB, lane 2: GSH + CDNB + KKSG6, lane 3: GSH + chloramphenicol + KKSG6, lane 4: GSH + chloramphenicol.

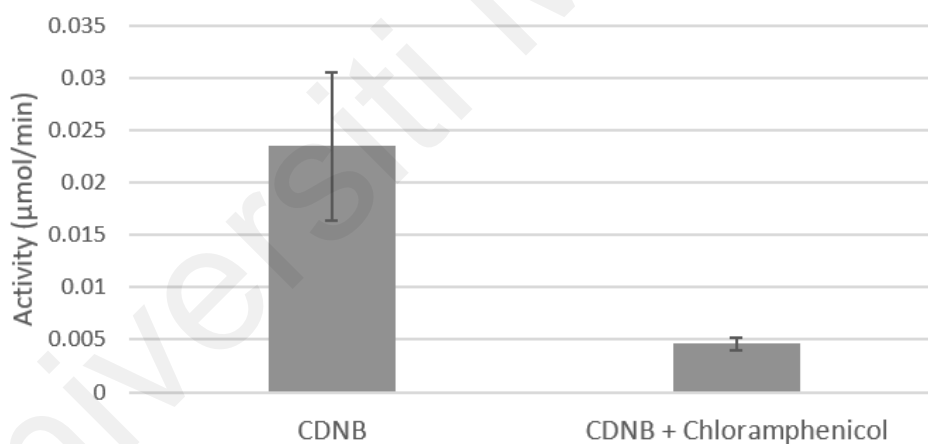


**Figure 4.16: KKSG6 assay with and without chloramphenicol**

The graph indicates the reduction of KKSG6 activity towards CDNB in the presence of chloramphenicol.

## 4.9 Molecular docking

Molecular docking was carried out following the steps explained in 3.2.12. Results for structure prediction and docking process are given in 4.9.1 and 4.9.2 respectively.

#### 4.9.1 Structure prediction

KKSG6 modelled 3D structure is given in **Figure 4.17**. The result of atom contacts and geometry analysis from modelled structure before and after refinement is summarised in **Table 4.1**.

**Table 4.1: Atom contacts and geometry analysis**

MolProbity parameter		Before refinement		After refinement	
All-atom contacts	Clashscore, all atoms	2.27		1.46	
Protein geometry	Poor rotamers	2	0.64%	0	0.00%
	Favored rotamers	297	95.19%	309	99.04%
	Ramachandran outliers	4	1.02%	2	0.51%
	Ramachandran favored	375	95.18%	381	96.70%
	Ramachandran distribution Z-score	1.01 $\pm$ 0.41		-0.28 $\pm$ 0.39	
	MolProbity score <sup>^</sup>	1.34		1.09	
	C $\beta$ deviations >0.25Å	2	0.53%	1	0.27%
	Bad bonds	0/3166	0.00%	0/3166	0.00%
	Bad angles	23/4320	0.53%	7/4320	0.16%
Peptide omegas	Cis Prolines	2/18	11.11%	2/18	11.11%
Low-resolution criteria	CaBLAM outliers	8	2.10%	10	2.60%
	CA Geometry outliers	3	0.77%	4	1.03%
Additional validations	Tetrahedral geometry outliers	1		0	
	Waters with clashes	0/0	0.00%	0/0	0.00%

In the two column results, the left column gives the raw count, right column gives the percentage.

<sup>^</sup>MolProbity score combines the clashscore, rotamer, and Ramachandran evaluations into a single score, normalized to be on the same scale as X-ray resolution.

#### 4.9.2 Protein-ligand docking

Binding of antibiotics within H-site and dimer interface of KKSG6 are successively visualised in **Figure 4.18** and **Figure 4.19**. **Table 4.2** summarises the interactions that occur in it.

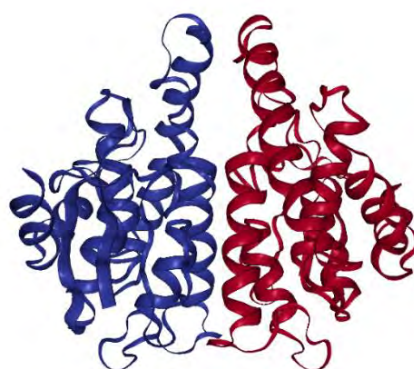


**Figure 4.17: KKSG6 3D structure model**

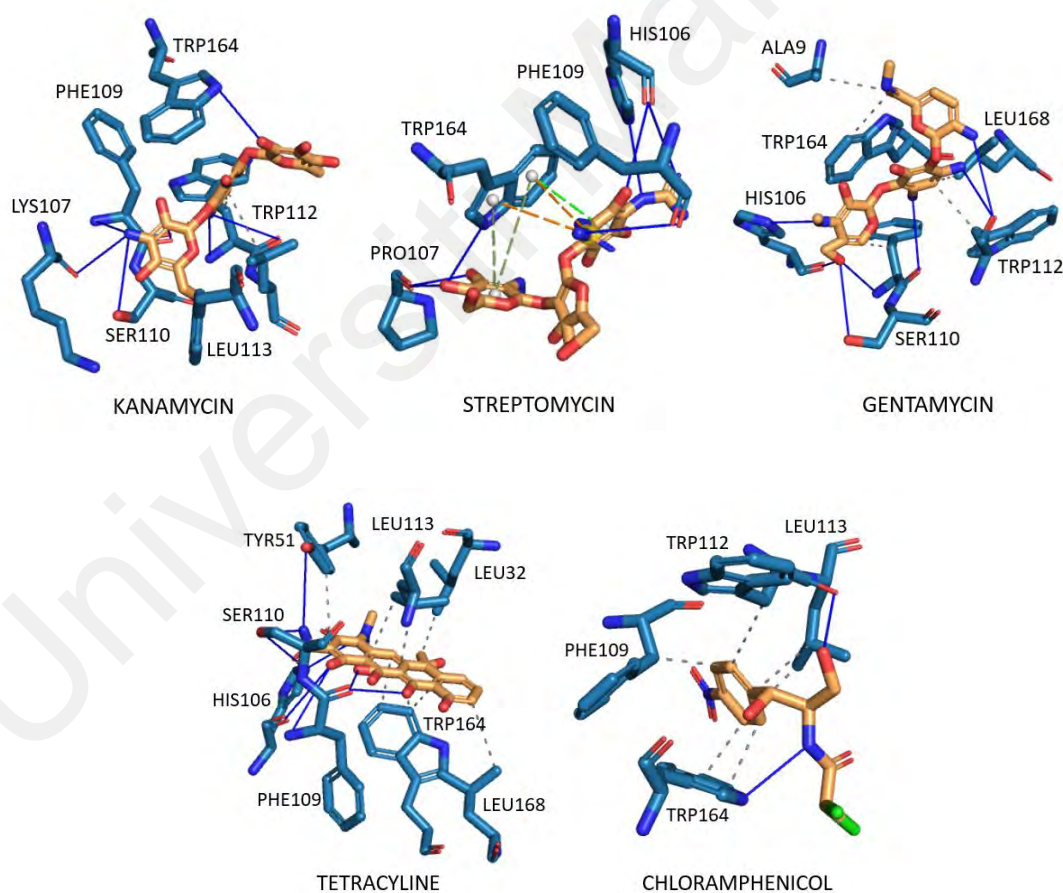


**Figure 4.18: Antibiotics binding within KKSG6 H-site**

Protein-ligands interactions are profiled using PLIP (<https://plip-tool.biotec.tu-dresden.de/plip-web/plip/index>). Blue line: hydrogen bond, Grey dash: hydrophobic interaction, Neon dash: pi stacking (parallel), Green dash: pi stacking (perpendicular), Orange dash: pi cation interaction, White ball: aromatic ring center.

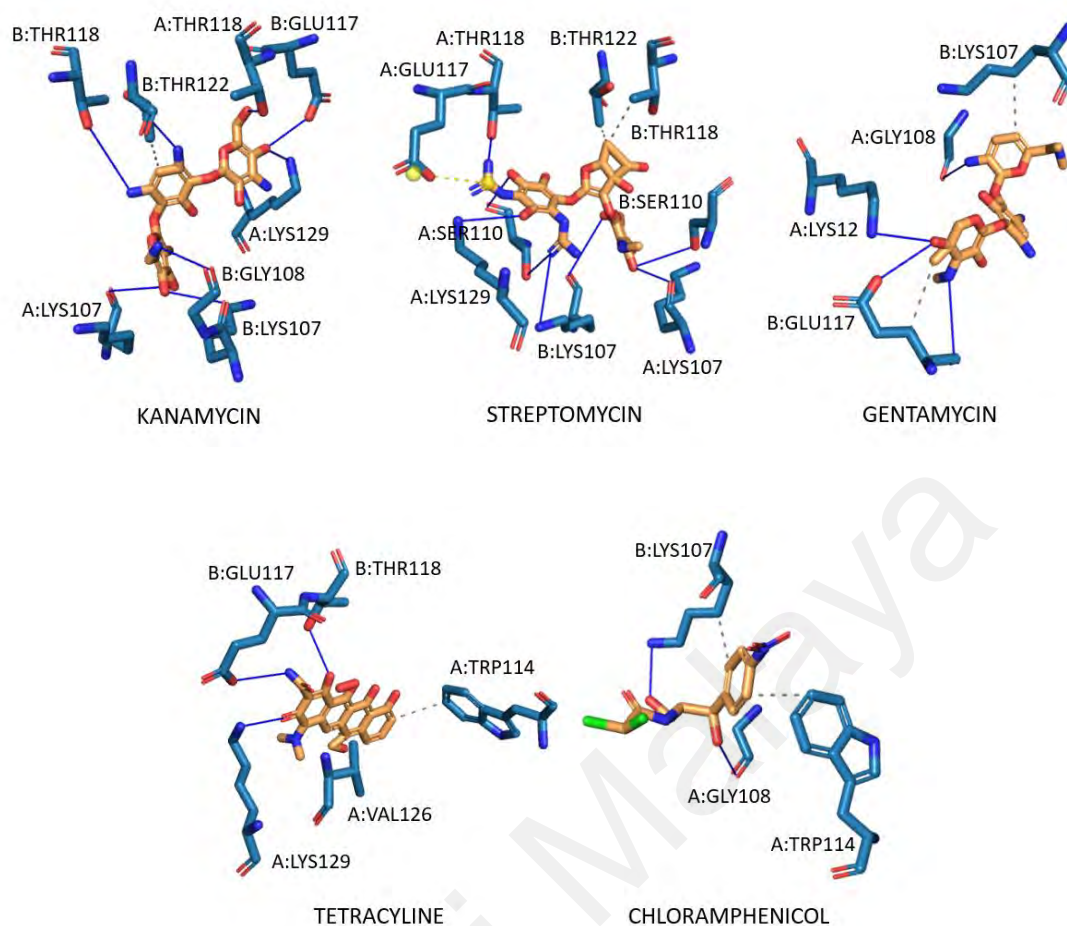


**Figure 4.19: Antibiotics binding within KKSG6 dimer interface**

Protein-ligands interactions are profiled using PLIP (<https://plip-tool.biotec.tu-dresden.de/plip-web/plip/index>). Blue line: hydrogen bond, Grey dash: hydrophobic interaction, Yellow dash: salt bridge, Yellow ball: charge.

**Table 4.2: KKSG6 interaction with antibiotics**

Location	Ligand	Binding energy^ (kcal/mol)	Inhibition constant^	Number of H bond	Number of salt bridge	No of hydrophobic interaction	No of pi orbital interaction	Amino acids involved in interaction□
Dimer interface	Kanamycin	-15.42	4.96 pM	9		1		A107Lys, B107Lys, B108Gly, B117Glu, A118Thr, B118Thr, B122Thr, A129Lys
	Streptomycin	-20.67	706.58 aM	8	1	2		A107Lys, B107Lys, A110Ser, B110Ser, B117Glu, A118Thr, B118Thr, B122Thr, A129Lys
	Gentamycin	-15.88	2.30 pM	4		2		B107Lys, A108Gly, B117Glu, A129Lys
	Tetracycline	-15.74	2.92 pM	4		2		A114Trp, B117Glu, B118Thr, A126Val, A129Lys
	Chloramphenicol	-5.95	43.53 uM	2		2		B107Lys, A108Gly, A114Trp
H-site	Kanamycin	-15.06	9.19 pM	8		2		51Tyr, 107Lys, 109Phe, 110Ser, 112Trp, 133Leu, 164Trp
	Streptomycin	-15.46	4.66 pM	7			4	7Pro, 106His, 109Phe, 164Trp
	Gentamycin	-14.21	38.21 pM	7		5		9Ala, 106His, 109Phe, 110Ser, 112Trp, 164Trp, 168Leu,
	Tetracycline	-17.74	99.90 fM	8		8		32Leu, 51Tyr, 106His, 109Phe, 110Ser, 113Leu, 164Trp, 168Leu
	Chloramphenicol	-5.93	45.34 uM	2		6		109Phe, 112Trp, 113Leu, 164Trp

^Estimated for temperature = 298.15 K

□A and B represent protein chains

T value = -0.881, significance = 0.428; T table for 90% confidence level and 4 degrees of freedom = 2.132

## CHAPTER 5:DISCUSSION

### 5.1 Bacterial retrieval

Bacterial retrieval was the first thing conducted in this research. In general, this process aimed to get the fresh bacterial culture from the frozen stock. *E. coli* BL21 Star™ (DE3) harbouring pET101/D-TOPO®-KKSG6 has been obtained in previous work (Shehu, 2018). The bacteria were preserved by freezing it in -80°C after it previously mixed with glycerol. Through doing so, the bacteria will last for several years and can be retrieved any time with a simple thawing procedure.

In this research, the *E. coli* BL21 Star™ (DE3) harbouring pET101/D-TOPO®-KKSG6 has been successfully retrieved with the procedure explained in 3.2.1 (see **Figure 4.1**). It is important to note that bacterial retrieval procedure that used in this research is the same routine procedure to culture the *E. coli*. However, since this bacteria strain carries the pET101/D-TOPO®-KKSG6 plasmid which contains ampicillin resistance gene, it is necessary to add ampicillin in the media to make sure that all bacteria that grew in the media is the one that carries the plasmid.

### 5.2 Bacterial validation

After the bacteria were retrieved, it is necessary to confirm whether the bacteria which grew in the plate were the right one that needed in this research. The validation was carried out by doing plasmid size and PCR analysis which further discussed in section 5.2.1 and 5.2.2.

### 5.2.1 Plasmid size analysis

To validate whether the retrieved bacteria were the one that carrying pET101/D-TOPO<sup>®</sup>-KKSG6, the plasmid contained inside the bacteria was isolated through the process called plasmid extraction. The size of this plasmid was then compared to the size of pET101/D-TOPO<sup>®</sup>-KKSG6. If they had the same size, then the plasmid inside the bacteria was most likely the wanted plasmid, pET101/D-TOPO<sup>®</sup>-KKSG6. However, if they had different size, the plasmid was exactly not the one that needed in this research.

The plasmid extraction was carried out following the procedure explained in 3.2.2.1.1. To confirm the success of extraction process, the plasmid was then electrophoresised in agarose gel matrix (see **Figure 4.2**). From the electrophoregram, it was observed there were three bands appeared: above 10 kb, around 6 kb and around 2 kb. According to De Mattos et al. (2004), there are three possible plasmid conformations namely supercoil, open circle and linear (see **Figure 5.1**).

Supercoil conformation is formed when both DNA strands are intact. It will create the compact 3D structure that moves rapidly under electrical current. Second conformation, an open circle, is a relaxed formed of plasmid that occurs when one of the DNA strands is broken. This conformation is slowly migrating during electrophoresis. The last conformation, a linear, is formed when both DNA strands breaks in the same position. The migration of linear plasmid is slower than supercoil and faster than open circle. Referring to the electrophoregram, the band which appeared on the top of the gel represented the open circle conformation of the plasmid. Meanwhile, the two bands that laid at around 6 kb and 2 kb were originated from the linear and supercoil conformation. Since the migration pattern of plasmid sample is consistent with the theoretical one, it can be assumed that the plasmid has been successfully isolated.

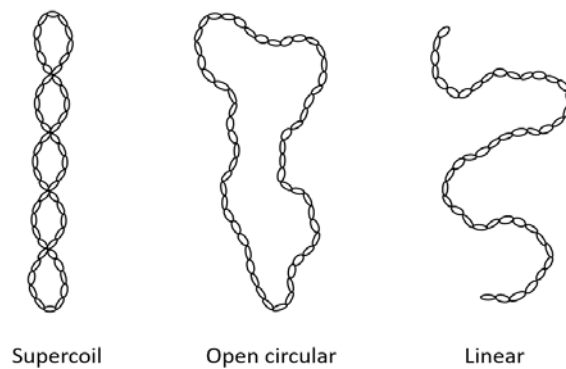


**Figure 5.1: Plasmid conformations**

To determine the size of previous isolated plasmid, the plasmid was electrophoresised together with the DNA ladder, a set of known-sized linear DNA that will separate through electrophoresis creating the ladder-like pattern. The size of the plasmid was determined by comparing its migration to the DNA ladder. However, the size comparison only valid if those DNA sample have the same conformation. Thus, the plasmid was first linearised by treating it with the restriction enzyme prior to electrophoresising.

The linearisation of the plasmid was conducted as explained in 3.2.2.1.2. Endonuclease *SacI*, with restriction site GAGCT<sup>^</sup>C, was utilised to cut both strands of plasmid. Since pET101/D-TOPO<sup>®</sup>-KKSG6 has only one *SacI* restriction site, linearisation of the plasmid should create the single linear DNA with size 6.4 kb. From the electrophoregram (see **Figure 4.3**), it was seen that after the linearisation, the plasmid also appeared as a single band at around 6 kb. The corresponding size between those two plasmids means that the previously isolated plasmid was most likely the one that needed in this research, pET101/D-TOPO<sup>®</sup>-KKSG6.

### 5.2.2 PCR analysis

PCR is a method to amplify the specific DNA sequence. It requires DNA polymerase, dNTPs, a pair of primers and DNA template. Basically, the idea of this PCR validation process was to confirm whether the isolated plasmid carrying the KKSG6 gene. To do so, the DNA template which required for amplification process came from the plasmid which had previously been isolated. And the primer used in PCR were those that only recognised the KKSG6 gene. If the KKSG6 gene contained within the plasmid, the PCR process will occur resulting the amplification of the KKSG6 gene. On the other hand, if the plasmid did not own the KKSG6 gene, the PCR will not work.

According to **Figure 4.4**, the negative control was clear from any bands, indicating no contamination occurred. The electrophoresis of the PCR mixture from plasmid sample exhibited the band between 500 bp and 700 bp. According to the database (see Appendix A), the size of KKSG6 gene is 609 bp. The consistency between PCR band size and the actual KKSG6 size implying the presence of KKSG6 gene in the plasmid sample. Thus, referring to the plasmid size analysis and PCR analysis, it can be concluded that the plasmid which had previously been isolated was most likely the pET101/D-TOPO<sup>®</sup>-KKSG6.

### 5.3 Expression of KKSG6

Gene expression refers to the process of protein production within the cells which involves DNA transcription, mRNA translation and protein modification. In this research, the expression of KKSG6 was carried out using pET101/D-TOPO<sup>®</sup>-KKSG6 as a vector and *E. coli* BL21 Star<sup>™</sup> (DE3) as a host. pET101/D-TOPO<sup>®</sup>-KKSG6 was designed to express the KKSG6 gene under T7 promoter that can only be recognised by bacteriophage T7 RNA polymerase. As previously stated in 3.1.4, *E. coli* BL21 Star<sup>™</sup> (DE3) as an expression host carried T7 RNA polymerase gene under the *lacUV5* promoter which can

be induced by isopropyl  $\beta$ -D-1-thiogalactopyranoside (IPTG). Thus, addition of IPTG to the cell culture will allow the expression of T7 RNA polymerase. This high activity and sensitivity polymerase will recognise T7 promoter within pET101/D-TOPO®-KKSG6, prompting the transcription of KKSG6 gene.

The expression of KKSG6 was conducted following the steps explained in 3.2.4. To confirm the success of expression process, a little amount of the cells was lysed by boiling it together with SDS-PAGE sample buffer. The total protein was then electrophoresed through polyacrylamide matrix following the procedure explained in 3.2.8.

As observed in **Figure 4.5**, the overall electrophoresis pattern before and after induction is similar, except the thick band at around 20 kDa which only appeared in the total protein sample after induction. According to the Compute pI/Mw ([https://web.expasy.org/compute\\_pi/](https://web.expasy.org/compute_pi/)), the molecular weight of KKSG6 is 22.14 kDa (Gasteiger et al., 2005). The consistency between observed band size and the theoretical KKSG6 size leads to the suggestion that the observed band around 20 kDa was most likely KKSG6. Thus, it can be concluded that the expression of KKSG6 has been successfully carried out.

#### **5.4 Optimisation expression of KKSG6**

The production of specific proteins within the organisms is mainly affected by the efficiency of transcription and translation process. How fast the mRNA could be synthesised, how stable it is against degradation and how it translated into protein are together regulating the amount of functional protein produced (Glick & Whitney, 1987; Slobodin et al., 2017). Technically, all those aspects involved in protein production can be simply tuned by changing the condition of protein expression. In this research, how

long the culture should be incubated and how much IPTG should be added to obtain the most functional protein were evaluated.

**Figure 4.6** represents the effect of post-induction incubation time on KKSG6 expression. Over time, the cell biomass tended to increase. From 4 up to 6 hours post-induction incubation, the total OD<sub>600</sub> was observed to be increasing. However, after 24 hours, the OD<sub>600</sub> was slightly drop. It corresponds with the typical bacterial growth which consist of several phases: lag, exponential, stationary and death. *E. coli* BL21 Star™ (DE3) harbouring pET101/D-TOPO®-KKSG6 is suggested to be in its exponential phase from 4 up to 6 hours after induction due to the continuous cell biomass increase. Meanwhile, because of there was slight decrease of cell biomass, the bacteria is predicted to be in the death phase after 24 hours post-induction.

On the contrary of cell biomass, the total activity of KKSG6 tended to decrease over time. The total activity was gradually increasing and reached its peak within 5 hours after the induction. It is proposed as a compensation from the rise of cell biomass. During the first 5 hours, the cells were actively dividing. The more cell observed, the more KKSG6 will be produced. However, the activity plunged for almost 65% after 24 hours post-induction. It might be caused by the protein degradation process inside the cells. When the culture was in late-exponential phase, the cells began to move into the stationary phase. During this period, the unnecessary proteins including KKSG6 were started to be degraded. The amino acids from degraded proteins were going to be reused in stationary phase to synthesise proteins required for survival: DNA repair, thermotolerance, osmotolerance, etc (Jaishankar & Srivastava, 2017).

The effect of IPTG concentration on KKSG6 expression is given in **Figure 4.7**. It is seen that the higher IPTG concentration added to induce the expression, the less biomass is produced, and the less total activity observed. It indicated that only small amount of IPTG was required for the expression to be induced. If the higher concentration of IPTG

was used, the cell division rate would drop due to pressure of expression process (Bentley et al., 1990; Dvorak et al., 2015). At some point, it even could be harmful for the cells, leading to the host death. In this study, the optimum IPTG concentration needed to induce the KKSG6 expression was 0.1 mM.

## 5.5 Bacterial cell lysis

Cell lysis refers to the process of cells membrane or wall disruption. Once the cell membrane or wall disrupted, all molecules inside the cells, including organelle, DNA, RNA and protein are released into the buffer. The solution which contains the cell contents that obtained from lysis process is called lysate. There are three types of cell lysis: physical, chemical and enzymatic. Physical lysis can be done by homogenisation, sonication and freeze-thaw. Chemically cell lysis usually done by treating the cells with detergent or alkaline. Meanwhile, enzymatic lysis conducted by treating the cells with enzyme, for example lysozyme, zymolase and cellulose. The advantages and disadvantages of each lysis type is summarised in **Table 5.1**.

In this research, the cell lysis was carried out chemically using CelLytic™ B (Sigma) as explained in 3.2.6. To verify the success of lysis process, both cell pellet and lysate fraction obtained from the centrifugation was electrophoresised. If the lysis was completely done, all the soluble protein will appear in lysate fraction, leaving only cell debris in the pellet. However, if the lysis did not occur, the cells will remain intact as a cell pellet, resulting the presence of protein bands in the pellet fraction.

The electrophoregram of cell lysis can be seen in **Figure 4.8**. It can be observed that protein bands appeared in both fractions. However, the intensity of the bands is much higher in lysate fraction than pellet. It means that the lysis process did occur, but it was not completely done. There was a little amount of bacterial cell which still intact, resulting

the presence of protein bands with low intensity. However, considering that only the small amount of the cells did not rupture, this lysis procedure was still employed in this research.

**Table 5.1: Three types of cell lysis comparison**

Advantage	Disadvantage
<b>Physical</b>	
<ul style="list-style-type: none"> <li>○ Can be used towards variety type of cells</li> <li>○ Force applied can be easily adjusted, leading to complete cell disruption</li> </ul>	<ul style="list-style-type: none"> <li>○ Harsh process, leading to protein denaturation and aggregation</li> <li>○ Expensive equipment is needed</li> <li>○ Reproducibility may vary, since there is no exact procedure of handling sample</li> </ul>
<b>Chemical</b>	
<ul style="list-style-type: none"> <li>○ Gentle method, resulting higher protein yield</li> <li>○ No expensive equipment required</li> </ul>	<ul style="list-style-type: none"> <li>○ The force cannot be adjusted easily, sometimes leads to incomplete cells disruption</li> <li>○ The cost for large-scale is expensive</li> <li>○ The presence of salts and detergents might affect downstream process</li> </ul>
<b>Enzymatic</b>	
<ul style="list-style-type: none"> <li>○ Gentle method, leading to higher protein yield</li> <li>○ No expensive equipment needed</li> </ul>	<ul style="list-style-type: none"> <li>○ The cost for large-scale is expensive</li> <li>○ Certain enzyme only can be used for certain type of cells</li> <li>○ The force cannot be adjusted easily, sometimes leads to incomplete cells disruption</li> </ul>

## 5.6 Protein purification

To carry out the functional studies of KKSG6, the pure protein is required. However, the lysate that obtained from previous step contains not only KKSG6 protein, but also other cell contents such as other proteins, DNA and RNA. Protein purification was basically done using affinity chromatography principle (see **Figure 3.4**). The lysate was

flowed through the column containing sepharose beads that has been engineered to link with the GSH, the GST substrate. As the lysate pass through the column, the KKSG6 will bind to the GSH and retain within the column. Meanwhile, other molecules that do not recognise the GSH will pass by. Once all the impurities pass by the column, the KKSG6 that remained in the column was released by flowing the high concentration of GSH.

The protein purification was carried out following the procedure in 3.2.7. The success of this process was validated by electrophoresising the eluted fraction (see **Figure 4.9**). There was only single band appeared in the eluted fraction, suggesting that the pure KKSG6 had been successfully obtained.

## 5.7 Antibiotic susceptibility testing

Beta class GST is known to play a role in the antibiotic resistance phenomenon. The interaction between beta class GST and antibiotics was first discovered when the presence of PmGST B1-1 *in vitro* was found to reduce the maximum inhibitory concentration of several antibiotics (Piccolomini et al., 1989). *In vivo* experiment also showed that under antibiotic stress, overexpressed-GST cells grew faster than control (Allocati et al., 1999). In this research, the interaction between KKSG6 and antibiotics has been evaluated.

The antibiotic susceptibility testing was carried out by comparing the growth of induced *E. coli* BL21 Star™ (DE3) containing pET101/D-TOPO®-KKSG6 and un-induced as a control, under various concentrations of antibiotics. According to the pharmacodynamics, there is a minimum concentration for the antibiotics to act against bacterial cells. Below that concentration, the presence of antibiotics is not considered enough to inhibit cell growth (Gullberg et al., 2011). Once the minimum concentration is reached, the inhibition growth of the cells will increase as the concentration rises. The

inhibition growth rise will then stop when it reaches its maximum, 100%, so the addition of antibiotics will no longer make a difference in cell inhibition growth. Referring to **Figure 4.10-14**, all antibiotics, except for chloramphenicol, exhibited the similar trend. Under kanamycin, streptomycin, gentamycin and tetracycline stress, the inhibition growth gradually increased with the rise of concentration. Meanwhile, when the bacterial cells were exposed to chloramphenicol, the inhibition percentage altered drastically from no to full inhibition within a narrow concentration range. This occurred because each antibiotic has a unique efficacy and dose response. Gentamycin and streptomycin have been reported to perform a low response towards bacterial cells. So, their concentration needs to be doubled at least 4 times to reach full inhibition growth (El-Halfawy & Valvano, 2013; Thiriard et al., 2020). Chloramphenicol, on the other hand, only requires 2 times two-fold serial dilution performed to go from complete to no inhibition at all (El-Halfawy & Valvano, 2013).

When the bacterial cells were exposed to 3.125-12.5 mg/L kanamycin (see **Figure 4.10**), the inhibition growth of *E. coli* containing KKSG6 was significantly lower than KKSG6 devoid *E. coli*. However, when the kanamycin concentration was raised to 25 and 50 mg/L, no significant inhibition growth observed between *E. coli* containing and lacking KKSG6. For streptomycin (see **Figure 4.11**), the inhibition percentage of KKSG6 devoid cells was significantly higher than the cells expressing KKSG6 within the range of 3.125-50 mg/L concentration, except for 12.5 mg/L. Under the exposure of 12.5 mg/L, the inhibition growth of those two cells was not considered to be statistically different due to a high error in the experiment. However, since the lower and higher concentrations showed the same trend, the growth inhibition of KKSG6 devoid cells under 12.5 mg/L streptomycin should also be considerably higher than the cells expressing KKSG6. The same thing also happened when the cells were subjected to tetracycline (see **Figure 4.13**). Under the exposure of 0.6125, 5 and 10 mg/L, the inhibition percentage of cells

containing KKSG6 was substantially lower than the control. Meanwhile, within the concentration range of 1.25-2.5 mg/L, the inhibition difference between those two cells was not considered to be significant, due to a high deviation in the data. However, since the lower and higher concentrations showed the same pattern, the cell inhibition growth without KKSG6 under 1.25-2.5 mg/L should also be considerably higher than the cells containing KKSG6. Under gentamycin stress (see **Figure 4.12**), statistical calculation revealed that the inhibition growth of *E. coli* expressing KKSG6 was significantly less than KKSG6 devoid *E. coli* within the concentration range of 1.25-10 mg/L. Under the lowest concentration, 0.625 mg/mL, the inhibition growth difference between cells containing KKSG6 and the control was not considered significant due to a high data uncertainty. However, since gentamycin exhibited the same pattern as the other antibiotics, the cells containing KKSG6 inhibition growth under 0.625 mg/L concentration should also be considerably lower than KKSG6 devoid cells. Within the exposure of 5 and 10 mg/L gentamycin, the paired T-test indicated that there was a significant inhibition growth difference between those two cells due to a small standard deviation. Nonetheless, the mean difference between sample and control under 5 and 10 mg/L gentamycin was relatively small in comparison to the other concentrations. Thus, the inhibition percentage difference between cells with and without KKSG6 under 5 and 10 mg/L gentamycin could be ignored. When the cells were treated with chloramphenicol (see **Figure 4.14**), the inhibition percentage of bacteria containing KKSG6 was observed to be significantly lower than KKSG6 devoid cells within the concentration range of 0.625-1.25 mg/L. Meanwhile, at the lower (0.3125 mg/L) and higher concentrations (2.5-5 mg/L) of chloramphenicol, the inhibition was not considered to be different.

In general, bacterial cell growth exhibited a similar pattern when exposed to kanamycin, gentamycin, streptomycin, tetracycline and chloramphenicol. In the concentration range where the inhibition growth increases with concentration, the

inhibition growth of bacterial cells containing KKSG6 is consistently lower than the control, indicating the involvement of KKSG6 in reducing the cells' susceptibility towards antibiotics. However, no significant difference in growth inhibition is observed at higher antibiotic concentrations (refer to Appendix C). It is then proposed that KKSG6 provides early protection for bacterial cells by interacting with the antibiotics.

## 5.8 Antibiotic conjugation study

Antibiotic susceptibility testing found that KKSG6 interaction with antibiotics could support bacterial cell survival under antibiotic exposure. However, how the interaction between beta class GST and antibiotics exactly forms has not been properly understood. Since GST is known as a conjugation enzyme, the protection provided by KKSG6 against antibiotic stress might come from its antibiotic conjugation activity. No one has ever reported the antibiotic conjugation activity of beta class GST, although the antibiotic conjugation performed by GST on various specimens, such as rat liver (Park & Choung, 2007), maize plant (Farkas et al., 2007), human fetal and neonatal liver (Holt et al., 1995) has been previously revealed. Thus, to understand the role of KKSG6 in antibiotic resistance development, the conjugation activity of KKSG6 towards antibiotics has been examined.

Thin layer chromatography analysis revealed an antibiotic conjugate spot within the chloramphenicol enzymatic mixture. However, the similar spot was not observed in kanamycin and tetracycline reactions (see **Figure 4.15**). It indicated that KKSG6 exhibits a conjugation reaction towards chloramphenicol, but not with the other two antibiotics. Evaluating the structure, the main characteristic differentiating chloramphenicol from other antibiotics, kanamycin and tetracycline, might be the size (see **Figure 5.2**). Chloramphenicol is smaller than kanamycin and tetracycline, so it could go into the H-site cavities easily and somehow occupy the site appropriately, allowing the conjugation

reaction to take place. Kanamycin and tetracycline, structure wise, are bulkier and more rigid, avoiding them from entering the H-site. Other distinct properties that could rationalise this phenomenon might come from the availability of weak bases as a leaving functional group within each antibiotic (see **Figure 5.2**). Beta class GST is known to exhibit low conjugation activity, even towards CDNB, the most common GST substrate (Perito et al., 1996; Shehu, 2018). On that basis, prior studies suggested beta class GST to facilitate a redox reaction as its *in vivo* main role rather than being a conjugation enzyme (Caccuri et al., 2002). Within the other GST classes, the conjugation reaction began with the activation of the thiol group by serine or tyrosine, resulting in the formation of the GS<sup>-</sup> ion, which was subsequently followed by a nucleophilic attack (see **Figure 2.4**) (Angelucci et al., 2005). However, the presence of cysteine residues in the beta class GST active sites rather than serine or tyrosine avoids the formation of GS<sup>-</sup> ion (Rossjohn et al., 1998). A kinetic evaluation of mutant PmGSTB1-1 also revealed that the cysteine residue was not essential for beta class conjugation activity (Caccuri et al., 2002). Thus, the reaction success is most likely determined by whether the co-substrate possesses a weak base functional group to be substituted by GSH. Since kanamycin and tetracycline have no weak base to act as a leaving group, no conjugation reaction occurred. Otherwise, the explanation might be simply because of tetracycline and kanamycin's inappropriate orientation in the H-site, which then prevents the conjugation reaction from taking place.

The GST assay with and without the presence of chloramphenicol was also performed to evaluate its inhibition effect (see **Figure 4.16**). As previously reported by Perito et al., (1996) that chloramphenicol reduced the PmGSTB1-1 activity, the same thing also happened to KKSG6. The KKSG6 conjugation activity towards CDNB plunged by 80%

in the presence of chloramphenicol, which most likely caused by the competition between CDNB and chloramphenicol to occupy the H-site.

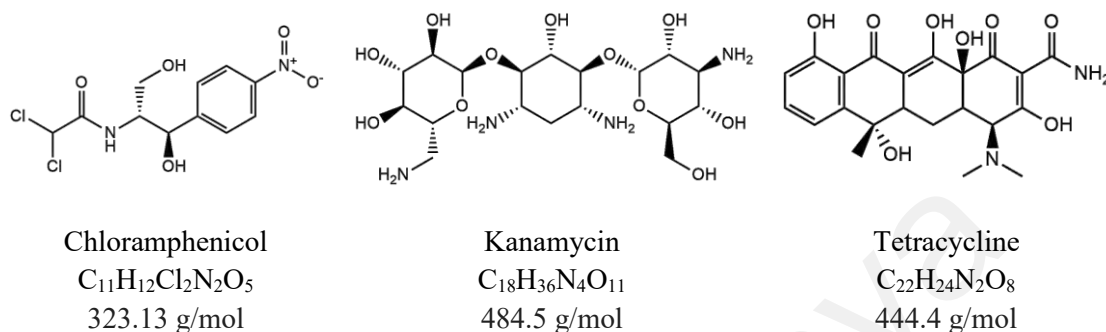


**Figure 5.2: Chloramphenicol, kanamycin and tetracycline structure comparison**

## 5.9 Molecular docking

Antibiotic susceptibility testing suggested that KKSG6 provides early protection for bacterial cells through binding with antibiotics. However, what kind of interaction occurs between them remains questionable since the antibiotic conjugation study revealed that KKSG6 could only exhibits conjugation activity towards chloramphenicol, and not with the other antibiotics. Previous research suggested two possible antibiotic binding sites, namely dimer interface and H-site. In this study, the preferred binding orientation of each antibiotic to both binding sites was predicted by molecular docking, which is further discussed in sections 5.9.1 and 5.9.2.

### 5.9.1 Structure prediction

Molecular docking is an *in-silico* study to predict the preferred orientation of ligand when attached to the protein. To do so, the protein structure is required as the input. Since

the KKSG6 structure is not available in the database, the structure was modelled following the details explained in 3.2.12.1.

The 3D structure of KKSG6 in this study was predicted through comparative modelling. This method constructs the target structure based on their amino acid sequence similarities with template, a closely related protein which quaternary structure has been solved. The principal of comparative modelling structure prediction relies on the fact that evolutionary related proteins with similar amino acid sequences also exhibit similar structures. Consequently, the higher sequence similarity between target and template protein, the better accuracy prediction will be obtained. It is widely accepted that a minimum 30% identity between target and template is required for this approach (Xiang, 2006). Aside from comparative homology modelling, the ab-initio approach which mainly relies on energy calculations can also be used to predict the protein structure. However, due to its ease and reliability, comparative modelling is the most common method to use in predicting protein quaternary structure. **Table 5.2** summarises the comparison of those methods.

**Table 5.2: Comparison between comparative and ab-initio modelling**

No	Distinguishing factor	Comparative modelling	Ab-initio modelling
1	Principal	Similar sequence means similar structure	The more stable structure the better
2	Process	Identify the amino acid sequence similarity and copy the structures	Generate a lot of possible structures and compared which one is the best
3	Knowledge	Protein structure and homology	Energy functions
4	Difficulty	Easy	Hard
5	Precision	Depend on the template	Good
6	Accuracy	Depend on the template	Might not be accurate

In this research, glutathione S-transferase from *Yersinia pestis* (PDB ID: 4GCI) with 49.75% identity and 1.5Å resolution was selected as a template. The result of modelled KKSG6 was then validated by examining its atomic interactions and geometry. According to MolProbity, the KKSG6 model still had some poor amino acid rotamers, Ramachandran outliers and bad bond angles (see **Table 4.1**). Thus, further refinement is required before the structure can be employed for molecular docking. A DeepRefiner server that is driven by deep network calibration was used to carry out the refinement process (Shuvo et al., 2021). The number of poor amino acid rotamers, Ramachandran outliers and bad bond angles were observed to decrease after refinement (see **Table 4.1**), indicating that the refinement process has successfully improved the quality of KKSG6 structure. Despite the fact that two Ramachandran outliers remained after the refinement procedure, the writer decided to neglect them due to their insignificance to the overall structure. Both Ramachandran outlier residues (Tyr175 in chains A and B) are positioned in the loop between  $\alpha 6$  and  $\alpha 7$ , which is far away from the docking sites, H-site and dimer interface (see **Figure 5.3**). The refined KKSG6 3D structure that was used for molecular docking is provided in **Figure 4.17**.

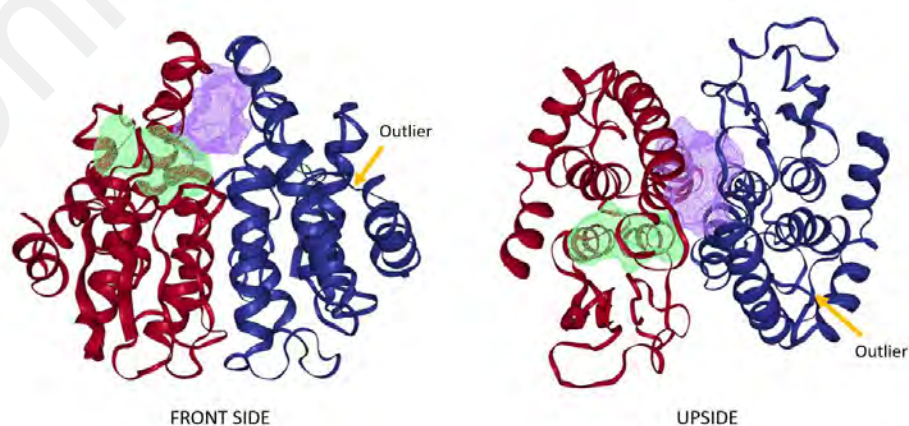


**Figure 5.3: Docking sites**

The figure was obtained from Proteins Plus (<https://proteins.plus/>). Purple surface: dimer interface, Green surface: H-site, Yellow arrow: Ramachandran outlier residue.

### 5.9.2 Protein-ligand docking

The preferred antibiotics conformation when bound to KKSG6 protein has been computationally simulated through protein-ligand docking. Study towards one of beta class GST, PmGSTB1-1, proposed H-site and dimer interface as two possible antibiotic binding sites (Rossjohn et al., 1998). Thus, KKSG6-antibiotic interaction in this study was investigated within those two possible sites (see **Figure 5.3**). Theoretically, the preferred ligand binding orientation to the protein could be determined by comparing the binding energy involved in the protein-ligand complex formation. The lower binding energy, the more likely binding will occur, and the more stable protein-ligand complex formed. Since no significant binding energy difference was observed between dimer interface and H-site (see **Table 4.2**), antibiotics appeared to have a similar affinity towards these two sites. It then suggested that antibiotics might be able to occupy both sites of the protein. Previous studies have proposed that antibiotic binding to the beta class GST takes place within dimer interface region due to the fact that: antibiotic binding to PmGSTB1-1, was observed to occur in a non-competitive manner (Allocati et al., 1999; Perito et al., 1996) and Trp164 residue, which is predicted to be involved in tetracycline and rifamycin binding within H-site region, was apparently not found to be necessary (Allocati et al., 2005). However, when a mixture of GSH, chloramphenicol and KKSG6 was analysed by thin layer chromatography, there was a GSH-chloramphenicol conjugate spot observed. It was indicated that chloramphenicol can also go into the H-site cavity of KKSG6, acting as a substrate for conjugation reaction. Some GSH-antibiotic conjugation activities of other GST classes, for example, GSH-chlortetracycline of maize GST (Farkas et al., 2007) and GSH-chloramphenicol of human fetal and neonatal liver GST (Holt et al., 1995), have also been reported. Although the antibiotics could bind to both dimer interface and H-site, the location preference where the antibiotics bind to the beta class GST seems like a structural-specific phenomenon.

Large antibiotics, such as tetracycline and rifamycin, would prefer to bind to a larger site, the dimer interface (Allocati et al., 2005). Molecular docking towards streptomycin, the bulkiest antibiotic tested in this study, also revealed that it binds to dimer interface better than to H-site (see **Table 4.2**). Meanwhile, small antibiotic with a weak base group like chloramphenicol would occupy the smaller cavity, H-site, undergoing the conjugation reaction with GSH. Besides from acting as a substrate, there is also a possibility where the antibiotics bind to the H-site without undergoing any conjugation reaction. Further study is obviously required to examine whether it is possible for each antibiotic to undergo conjugation reaction while sitting on the H-site.

Besides binding energy, the other information that could be obtained from protein-ligand docking is the inhibition constant, which refers to the concentration required to produce half of the maximum inhibition. The inhibition constant reflects how effective the ligand is as an inhibitor. The lower inhibition constant, the more potential inhibitors the ligand. Molecular docking between KKSG6 and antibiotics indicated that streptomycin and tetracycline are the most powerful inhibitors since they gave the lowest inhibition constant among other antibiotics. Chloramphenicol, on the other hand, most likely did not act as an inhibitor due to its high inhibition constant (refer **Table 4.2**). It is also supported by a previous antibiotic inhibition study of PmGSTB1-1 which found that the concentration of tetracycline required to inhibit 50% of activity is much lower than chloramphenicol and the other antibiotics tested, making tetracycline the strongest inhibitor among other antibiotics (Perito et al., 1996).

## CHAPTER 6: CONCLUSION

### 6.1 Conclusion

A study of antibiotic resistance developed by beta class GST using one of the GST isozymes found in *Acidovorax* sp. KKS102, KKSG6, has been carried out. The following conclusions have been made:

- a. KKSG6 has successfully been expressed in *E. coli* BL21 Star™ (DE3) using pET101/D-TOPO®-KKSG6 as an expression vector,
- b. The optimum expression level of KKSG6 was achieved when the culture was incubated for 5 hours after the addition of 0.1 mM IPTG,
- c. KKSG6 has been purified using GSTrap™ HP column,
- d. Over-expression of KKSG6 made the bacterial cells less susceptible towards antibiotics, suggesting the antibiotics binding with KKSG6,
- e. KKSG6 conjugation activity towards chloramphenicol, that could also act as an inhibitor, has been demonstrated,
- f. Molecular docking proposed that KKSG6-antibiotics binding could take place at the protein dimer interface and H-site depending on their properties.

### 6.2 Future work

Antibiotic susceptibility testing, antibiotic conjugation study and molecular docking have suggested that antibiotic binding could take place at KKSG6 dimer interface and H-site depending on their properties. However, further studies are required to support this finding. Other molecular docking should be performed to evaluate the interaction between GSH in the G-site and antibiotics in the H-site to gain a better understanding of why some antibiotics can undergo conjugation reactions, but others cannot. It is also important to validate which residues are necessary for antibiotic binding, which could be

accomplished by site-directed mutagenesis. Otherwise, a crystallographic analysis of antibiotic-KKSG6 complex might be the best way to confirm this hypothesis.

Universiti Malaya

## REFERENCES

- Adasme, M. F., Linnemann, K. L., Bolz, S. N., Kaiser, F., Salentin, S., Haupt, V. J., & Schroeder, M. (2021). PLIP 2021: Expanding the scope of the protein–ligand interaction profiler to DNA and RNA. *Nucleic Acids Research*, 49(W1), W530–W534.
- Allocati, N., Casalone, E., Masulli, M., Ceccarelli, I., Carletti, E., Parker, M. W., & Di Ilio, C. (1999). Functional analysis of the evolutionarily conserved proline 53 residue in *Proteus mirabilis* glutathione transferase B1-1. *FEBS Letters*, 445(2–3), 347–350.
- Allocati, N., Cellini, L., Aceto, A., Iezzi, T., Angelucci, S., Robuffo, I., & Di Ilio, C. (1994). Immunogold localization of glutathione transferase B1-1 in *Proteus mirabilis*. *FEBS Letters*, 354(2), 191–194.
- Allocati, N., Favalaro, B., Masulli, M., Alexeyev, M. F., & Di Ilio, C. (2003). *Proteus mirabilis* glutathione S-transferase B1-1 is involved in protective mechanisms against oxidative and chemical stresses. *Biochemical Journal*, 373(1), 305–311.
- Allocati, N., Federici, L., Masulli, M., & Di Ilio, C. (2009). Glutathione transferases in bacteria. *FEBS Journal*, 276(1), 58–75.
- Allocati, N., Federici, L., Masulli, M., & Di Ilio, C. (2012). Distribution of glutathione transferases in Gram-positive bacteria and archaea. *Biochimie*, 94(3), 588–596.
- Allocati, N., Masulli, M., Pietracupa, M., Favalaro, B., Federici, L., & Di Ilio, C. (2005). Contribution of the two conserved tryptophan residues to the catalytic and structural properties of *Proteus mirabilis* glutathione S-transferase B1-1. *Biochemical Journal*, 385(1), 37–43.
- Aminov, R. I. (2009). The role of antibiotics and antibiotic resistance in nature. *Environmental Microbiology*, 11(12), 2970–2988.
- Aminov, R. I. (2010). A brief history of the antibiotic era: Lessons learned and challenges for the future. *Frontiers in Microbiology*, 1(DEC), 1–7.
- Angelucci, F., Baiocco, P., Brunori, M., Gourlay, L., Morea, V., & Bellelli, A. (2005). Insights into the catalytic mechanism of glutathione S-transferase: The lesson from *Schistosoma haematobium*. *Structure*, 13(9), 1241–1246.
- Axarli, I. A., Rigden, D. J., & Labrou, N. E. (2004). Characterization of the ligandin site of maize glutathione S-transferase I. *Biochemical Journal*, 382(3), 885–893.
- Ayala, A., Muñoz, M. F., & Argüelles, S. (2014). Lipid Peroxidation: Production, metabolism, and signaling mechanisms of malondialdehyde and 4-hydroxy-2-nonenal. *Oxidative Medicine and Cellular Longevity*, 2014, 1–31.
- Bader, R., & Leisinger, T. (1994a). Isolation and characterization of the *Methylophilus* sp. strain DM11 gene encoding dichloromethane dehalogenase/glutathione S-transferase. *Journal of Bacteriology*, 176(12), 3466–3473.
- Bader, R., & Leisinger, T. (1994b). Isolation and characterization of the *Methylophilus* sp. strain DM11 gene encoding dichloromethane dehalogenase/glutathione S-transferase. *Journal of Bacteriology*, 176(12), 3466–3473.

- Belchik, S. M., & Xun, L. (2011). S-glutathionyl-(chloro)hydroquinone reductases: A new class of glutathione transferases functioning as oxidoreductases. *Drug Metabolism Reviews*, 43(2), 307–316.
- Bentley, W. E., Mirjalili, N., Andersen, D. C., Davis, R. H., & Kompala, D. S. (1990). Plasmid-encoded protein: The principal factor in the “metabolic burden” associated with recombinant bacteria. *Biotechnology and Bioengineering*, 35(7), 668–681.
- Bertoni, M., Kiefer, F., Biasini, M., Bordoli, L., & Schwede, T. (2017). Modeling protein quaternary structure of homo- and hetero-oligomers beyond binary interactions by homology. *Scientific Reports*, 7(1), 1–15.
- Board, P. G., Coggan, M., Wilce, M. C. J., & Parker, M. W. (1995). Evidence for an essential serine residue in the active site of the theta class glutathione transferases. *Biochemical Journal*, 311(1), 247–250.
- Board, Philip G., Baker, R. T., Chelvanayagam, G., & Jermini, L. S. (1997). Zeta, a novel class of glutathione transferases in a range of species from plants to humans. *Biochemical Journal*, 328(3), 929–935.
- Brown, A. P., & Gandolfi, A. J. (1994). Glutathione-S-transferase is a target for covalent modification by a haloethane reactive intermediate in the guinea pig liver. *Toxicology*, 89(1), 35–47.
- Burmeister, A. R. (2015). Horizontal gene transfer. *Evolution, Medicine, and Public Health*, 2015(1), 193–194.
- Bush, K., Courvalin, P., Dantas, G., Davies, J., Eisenstein, B., Huovinen, P., Jacoby, G. A., Kishony, R., Kreiswirth, B. N., Kutter, E., Lerner, S. A., Levy, S., Lewis, K., Lomovskaya, O., Miller, J. H., Mobashery, S., Piddock, L. J. V., Projan, S., Thomas, C. M., ... Zgurskaya, H. I. (2011). Tackling antibiotic resistance. *Nature Reviews Microbiology*, 9(12), 894–896.
- Caccuri, A. M., Antonini, G., Allocati, N., Di Ilio, C., Innocenti, F., De Maria, F., Parker, M. W., Masulli, M., Polizio, F., Federici, G., & Ricci, G. (2002). Properties and utility of the peculiar mixed disulfide in the bacterial glutathione transferase B 1-1. *Biochemistry*, 41(14), 4686–4693.
- Caccuri, A. M., Antonini, G., Allocati, N., Ilio, C. Di, De Maria, F., Innocenti, F., Parker, M. W., Masulli, M., Bello, M. Lo, Turella, P., Federici, G., & Riccia, G. (2002). GSTB1-1 from *Proteus mirabilis*: A snapshot of an enzyme in the evolutionary pathway from a redox enzyme to a conjugating enzyme. *Journal of Biological Chemistry*, 277(21), 18777–18784.
- Caccuri, A. M., Antonini, G., Nicotra, M., Battistoni, A., Bello, M. Lo, Board, P. G., Parker, M. W., & Ricci, G. (1997). Catalytic mechanism and role of hydroxyl residues in the active site of theta class glutathione S-transferases - Investigation of Ser-9 and Tyr-113 in a glutathione S-transferase from the Australian sheep blowfly, *Lucilia cuprina*. *Journal of Biological Chemistry*, 272(47), 29681–29686.
- Campbell, E. A., Korzheva, N., Mustaev, A., Murakami, K., Nair, S., Goldfarb, A., & Darst, S. A. (2001). Structural mechanism for rifampicin inhibition of bacterial RNA polymerase. *Cell*, 104(6), 901–912.

- Capasso, C., & Supuran, C. T. (2014). Sulfa and trimethoprim-like drugs – antimetabolites acting as carbonic anhydrase, dihydropteroate synthase and dihydrofolate reductase inhibitors. *Journal of Enzyme Inhibition and Medicinal Chemistry*, 29(3), 379–387.
- Centers for Disease Control. (2019). *Antibiotic Resistance Threats in the United States, 2019*.
- Chen, H., & Juchau, M. R. (1997). Glutathione S-transferases act as isomerases in isomerization of 13-cis-retinoic acid to all-trans-retinoic acid in vitro. *Biochemical Journal*, 327(3), 721–726.
- Chopra, I., & Roberts, M. (2001). Tetracycline antibiotics: Mode of action, applications, molecular biology, and epidemiology of bacterial resistance. *Microbiology and Molecular Biology Reviews*, 65(2), 232–260.
- Dahl, E. L., Shock, J. L., Shenai, B. R., Gut, J., DeRisi, J. L., & Rosenthal, P. J. (2006). Tetracyclines specifically target the apicoplast of the malaria parasite *Plasmodium falciparum*. *Antimicrobial Agents and Chemotherapy*, 50(9), 3124–3131.
- Das, B. C., Thapa, P., Karki, R., Das, S., Mahapatra, S., Liu, T.-C., Torregroza, I., Wallace, D. P., Kambhampati, S., Van Veldhuizen, P., Verma, A., Ray, S. K., & Evans, T. (2014). Retinoic acid signaling pathways in development and diseases. *Bioorganic & Medicinal Chemistry*, 22(2), 673–683.
- Dasari, S. (2017). Glutathione S-transferases detoxify endogenous and exogenous toxic agents - Minireview. *Journal of Dairy, Veterinary & Animal Research*, 5(5), 3–6.
- Davies, J., & Davies, D. (2010). Origins and evolution of antibiotic resistance. *Microbiology and Molecular Biology Reviews*, 74(3), 417–433.
- De Mattos, J. C. P., Dantas, F. J. S., Caldeira-De-Araújo, A., & Moraes, M. O. (2004). Agarose gel electrophoresis system in the classroom: Detection of DNA strand breaks through the alteration of plasmid topology. *Biochemistry and Molecular Biology Education*, 32(4), 254–257.
- Di Ilio, C., Aceto, A., Piccolomini, R., Allocati, N., Faraone, A., Cellini, L., Ravagnan, G., & Federici, G. (1988). Purification and characterization of three forms of glutathione transferase from *Proteus mirabilis*. *Biochemical Journal*, 255(3), 971–975.
- Doronina, N. V., Braus-Stromeier, S. A., Leisinger, T., & Trotsenko, Y. A. (1995). Isolation and characterization of a new facultatively methylotrophic bacterium: Description of *Methylophaga multivorans*, gen. nov., sp. nov. *Systematic and Applied Microbiology*, 18(1), 92–98.
- Dourado, D., Fernandes, P., & Ramos, M. (2008). Mammalian cytosolic glutathione transferases. *Current Protein & Peptide Science*, 9(4), 325–337.
- Dvorak, P., Chrast, L., Nikel, P. I., Fedr, R., Soucek, K., Sedlackova, M., Chaloupkova, R., de Lorenzo, V., Prokop, Z., & Damborsky, J. (2015). Exacerbation of substrate toxicity by IPTG in *Escherichia coli* BL21(DE3) carrying a synthetic metabolic pathway. *Microbial Cell Factories*, 14(1), 1–15.
- El-Halfawy, O. M., & Valvano, M. A. (2013). Chemical communication of antibiotic resistance by a highly resistant subpopulation of bacterial cells. *PLoS ONE*, 8(7), 1–10.

- Elshamy, A. A., & Aboshanab, K. M. (2020). A review on bacterial resistance to carbapenems: epidemiology, detection and treatment options. *Future Science OA*, 6(3), 1–15.
- Evans, G. J., Ferguson, G. P., Booth, I. R., & Vuilleumier, S. (2000). Growth inhibition of *Escherichia coli* by dichloromethane in cells expressing dichloromethane dehalogenase/glutathione S-transferase. *Microbiology*, 146(11), 2967–2975.
- Farkas, M., Berry, J. O., & Aga, D. S. (2007). Determination of enzyme kinetics and glutathione conjugates of chlortetracycline and chloroacetanilides using liquid chromatography-mass spectrometry. *Analyst*, 132(7), 664–671.
- Federici, L., Masulli, M., Di Ilio, C., & Allocati, N. (2010). Characterization of the hydrophobic substrate-binding site of the bacterial beta class glutathione transferase from *Proteus mirabilis*. *Protein Engineering, Design and Selection*, 23(9), 743–750.
- Fortin, P. D., Horsman, G. P., Yang, H. M., & Eltis, L. D. (2006). A glutathione S-transferase catalyzes the dehalogenation of inhibitory metabolites of polychlorinated biphenyls. *Journal of Bacteriology*, 188(12), 4424–4430.
- Frère, J. M., Joris, B., & Shockman, G. D. (1984). Penicillin-sensitive enzymes in peptidoglycan biosynthesis. *CRC Critical Reviews in Microbiology*, 11(4), 299–396.
- Frieri, M., Kumar, K., & Boutin, A. (2017). Antibiotic resistance. *Journal of Infection and Public Health*, 10(4), 369–378.
- Gasteiger, E., Hoogland, C., Gattiker, A., Duvaud, S., Wilkins, M. R., Appel, R. D., & Bairoch, A. (2005). Protein identification and analysis tools on the ExPASy server. In *The Proteomics Protocols Handbook* (pp. 571–607). Humana Press.
- Glick, B. R., & Whitney, G. K. (1987). Factors affecting the expression of foreign proteins in *Escherichia coli*. *Journal of Industrial Microbiology*, 1(5), 277–282.
- Gould, K. (2016). Antibiotics: from prehistory to the present day. *Journal of Antimicrobial Chemotherapy*, 71(3), 572–575.
- Green, A. R., Hayes, R. P., Xun, L., & Kang, C. H. (2012). Structural understanding of the glutathione-dependent reduction mechanism of glutathionyl-hydroquinone reductases. *Journal of Biological Chemistry*, 287(43), 35838–35848.
- Gullberg, E., Cao, S., Berg, O. G., Ilbäck, C., Sandegren, L., Hughes, D., & Andersson, D. I. (2011). Selection of resistant bacteria at very low antibiotic concentrations. *PLoS Pathogens*, 7(7).
- Habig, W. H., Pabst, M. J., & Jakoby, W. B. (1974). Glutathione S-transferases. The first enzymatic step in mercapturic acid formation. *The Journal of Biological Chemistry*, 249(22), 7130–7139.
- Holt, D. E., Hurley, R., & Harvey, D. (1995). Metabolism of chloramphenicol by glutathione S-transferase in human fetal and neonatal liver. *Neonatology*, 67(4), 230–239.
- Hossain, M. Z., Teixeira da Silva, J. A., & Fujita, M. (2006). Differential roles of glutathione S-transferases in oxidative stress modulation. *Floriculture, Ornamental and Plant Biotechnology. Advances and Topical Issues*, 3(December), 108–116.
- Huang, Y., Xun, R., Chen, G., & Xun, L. (2008). Maintenance role of a glutathionyl-hydroquinone lyase (PcpF) in pentachlorophenol degradation by *Sphingobium chlorophenolicum* ATCC 39723. *Journal of Bacteriology*, 190(23), 7595–7600.

- Hutchings, M., Truman, A., & Wilkinson, B. (2019). Antibiotics: past, present and future. *Current Opinion in Microbiology*, 51, 72–80.
- Jaishankar, J., & Srivastava, P. (2017). Molecular basis of stationary phase survival and applications. *Frontiers in Microbiology*, 8, 1–12.
- Jakoby, W. B., & Keen, J. H. (1977). A triple-threat in detoxification: The glutathione S-transferases. *Trends in Biochemical Sciences*, 2(10), 229–231.
- Jorgensen, J. H., & Ferraro, M. J. (2009). Antimicrobial susceptibility testing: A review of general principles and contemporary practices. *Clinical Infectious Diseases*, 49(11), 1749–1755.
- Kayser, M. F., & Vuilleumier, S. (2001). Dehalogenation of dichloromethane by dichloromethane dehalogenase/glutathione S-transferase leads to formation of DNA adducts. *Journal of Bacteriology*, 183(17), 5209–5212.
- Khan, S. N., & Khan, A. U. (2016). Breaking the spell: Combating multidrug resistant ‘Superbugs’. *Frontiers in Microbiology*, 7(FEB), 1–11.
- Kiefer, P. M., McCarthy, D. L., & Copley, S. D. (2002). The reaction catalyzed by tetrachlorohydroquinone dehalogenase does not involve nucleophilic aromatic substitution. *Biochemistry*, 41(4), 1308–1314.
- Kohler-Staub, D., & Leisinger, T. (1985). Dichloromethane dehalogenase of *Hyphomicrobium* sp. strain DM2. *Journal of Bacteriology*, 162(2), 676–681.
- Kontur, W. S., Bingman, C. A., Olmsted, C. N., Wassarman, D. R., Ulbrich, A., Gall, D. L., Smith, R. W., Yusko, L. M., Fox, B. G., Noguera, D. R., Coon, J. J., & Donohue, T. J. (2018). *Novosphingobium aromaticivorans* uses a Nu-class glutathione S-transferase as a glutathione lyase in breaking the  $\beta$ -aryl ether bond of lignin. *Journal of Biological Chemistry*, 293(14), 4955–4968.
- Kontur, W. S., Olmsted, C. N., Yusko, L. M., Niles, A. V., Walters, K. A., Beebe, E. T., Vander Meulen, K. A., Karlen, S. D., Gall, D. L., Noguera, D. R., & Donohue, T. J. (2019). A heterodimeric glutathione S-transferase that stereospecifically breaks lignin’s (R)-aryl ether bond reveals the diversity of bacterial  $\beta$ -etherases. *Journal of Biological Chemistry*, 294(6), 1877–1890.
- La Roche, S. D., & Leisinger, T. (1991). Identification of dcmR, the regulatory gene governing expression of dichloromethane dehalogenase in *Methylobacterium* sp. strain DM4. *Journal of Bacteriology*, 173(21), 6714–6721.
- Litwack, G., Ketterer, B., & Arias, I. M. (1971). Ligandin: A hepatic protein which binds steroids, bilirubin, carcinogens and a number of exogenous organic anions. *Nature*, 234(5330), 466–467.
- Lloyd-Jones, G., & Lau, P. C. K. (1997). Glutathione S-transferase-encoding gene as a potential probe for environmental bacterial isolates capable of degrading polycyclic aromatic hydrocarbons. *Applied and Environmental Microbiology*, 63(8), 3286–3290.
- Lu, S. C. (2009). Regulation of glutathione synthesis. *Molecular Aspects of Medicine*, 30(1–2), 42–59.
- Maclean, R. C., Hall, A. R., Perron, G. G., & Buckling, A. (2010). The evolution of antibiotic resistance: insight into the roles of molecular mechanisms of resistance and treatment context. *Discovery Medicine*, 10(51), 112–118.

- Marsh, M., Shoemark, D. K., Jacob, A., Robinson, C., Cahill, B., Zhou, N. Y., Williams, P. A., & Hadfield, A. T. (2008). Structure of bacterial glutathione-S-transferase maleyl pyruvate isomerase and implications for mechanism of isomerisation. *Journal of Molecular Biology*, 384(1), 165–177.
- Martínez-Márquez, A., Martínez-Esteso, M. J., Vilella-Antón, M. T., Sellés-Marchart, S., Morante-Carriel, J. A., Hurtado, E., Palazon, J., & Bru-Martínez, R. (2017). A tau class glutathione-S-transferase is involved in trans-resveratrol transport out of grapevine cells. *Frontiers in Plant Science*, 8, 1457.
- Masai, E., Ichimura, A., Sato, Y., Miyauchi, K., Katayama, Y., & Fukuda, M. (2003). Roles of the enantioselective glutathione S -transferases in cleavage of  $\beta$ -aryl ether. *Journal of Bacteriology*, 185(6), 1768–1775.
- McCarthy, D. L., Louie, D. F., & Copley, S. D. (1997). Identification of a covalent intermediate between glutathione and cysteine13 formed during catalysis by tetrachlorohydroquinone dehalogenase. *Journal of the American Chemical Society*, 119(46), 11337–11338.
- Meux, E., Prosper, P., Ngadin, A., Didierjean, C., Morel, M., Dumarçay, S., Lamant, T., Jacquot, J. P., Favier, F., & Gelhaye, E. (2011). Glutathione transferases of *Phanerochaete chrysosporium*: S-glutathionyl-p-hydroquinone reductase belongs to a new structural class. *Journal of Biological Chemistry*, 286(11), 9162–9173.
- Mignogna, G., Allocati, N., Aceto, A., Piccolomini, R., Di Ilio, C., Barra, D., & Martini, F. (1993). The amino acid sequence of glutathione transferase from *Proteus mirabilis*, a prototype of a new class of enzymes. *European Journal of Biochemistry*, 211(3), 421–425.
- Mitchell, A. E., Morin, D., Lame, M. W., & Jones, A. D. (1995). Purification, mass spectrometric characterization, and covalent modification of murine glutathione S-transferases. *Chemical Research in Toxicology*, 8(8), 1054–1062.
- Morgenstern, R., Depierre, J. W., & Ernster, L. (1979). Activation of microsomal glutathione S-transferase activity by sulfhydryl reagents. *Biochemical and Biophysical Research Communications*, 87(3), 657–663.
- Morgenstern, R., Zhang, J., & Johansson, K. (2011). Microsomal glutathione transferase 1: Mechanism and functional roles. *Drug Metabolism Reviews*, 43(2), 300–306.
- Morris, G. M., Ruth, H., Lindstrom, W., Sanner, M. F., Belew, R. K., Goodsell, D. S., & Olson, A. J. (2009). Software news and updates AutoDock4 and AutoDockTools4: Automated docking with selective receptor flexibility. *Journal of Computational Chemistry*, 30(16), 2785–2791.
- Muleta, A. W. (2016). *Glutathione transferases as detoxification agents: Structural and functional studies*. (Doctoral dissertation, University of Turku). Retrieved from <https://www.utupub.fi/handle/10024/124698?show=full>
- O'Neill, J. (2016). *Tackling drug-resistant infections globally: Final report and recommendations - The review on antimicrobial resistance; 2016*.
- Pajaud, J., Kumar, S., Rauch, C., Morel, F., & Aninat, C. (2012). Regulation of signal transduction by glutathione transferases. *International Journal of Hepatology*, 2012(2), 1–11.

- Pandey, T., Chhetri, G., Chinta, R., Kumar, B., Singh, D. B., Tripathi, T., & Singh, A. K. (2015). Functional classification and biochemical characterization of a novel rho class glutathione S -transferase in *Synechocystis* PCC 6803. *FEBS Open Bio*, 5(1), 1–7.
- Pandey, T., Singh, S. K., Chhetri, G., Tripathi, T., & Singh, A. K. (2015). Characterization of a highly pH stable Chi-class glutathione S-transferase from *Synechocystis* PCC 6803. *PLoS ONE*, 10(5), 1–15.
- Papp-Wallace, K. M., Endimiani, A., Taracila, M. A., & Bonomo, R. A. (2011). Carbapenems: Past, present, and future. *Antimicrobial Agents and Chemotherapy*, 55(11), 4943–4960.
- Park, H., & Choung, Y. K. (2007). Degradation of antibiotics (tetracycline, sulfathiazole, ampicillin) using enzymes of glutathion S-transferase. *Human and Ecological Risk Assessment*, 13(5), 1147–1155.
- Pemble, S. E., Wardle, A. F., & Taylor, J. B. (1996). Glutathione S-transferase class kappa: Characterization by the cloning of rat mitochondrial GST and identification of a human homologue. *Biochemical Journal*, 319(3), 749–754.
- Perito, B., Allocati, N., Casalone, E., Masulli, M., Dragani, B., Polsinelli, M., Aceto, A., & Ilio, C. Di. (1996). Molecular cloning and overexpression of a glutathione transferase gene from *Proteus mirabilis*. *Biochemical Journal*, 318(1), 157–162.
- Piccolomini, R., Di Ilio, C., Aceto, A., Allocati, N., Faraone, A., Cellini, L., Ravagnan, G., & Federici, G. (1989). Glutathione transferase in bacteria: Subunit composition and antigenic characterization. *Journal of General Microbiology*, 135(11), 3119–3125.
- Raza, H. (2011). Dual localization of glutathione S-transferase in the cytosol and mitochondria: implications in oxidative stress, toxicity and disease. *FEBS Journal*, 278(22), 4243–4251.
- Rogers, M. E., Jani, M. K., & Vogt, R. G. (1999). An olfactory-specific glutathione-S-transferase in the sphinx moth *Manduca sexta*. *The Journal of Experimental Biology*, 202(12), 1625–1637.
- Rossjohn, J., Polekhina, G., Feil, S. C., Allocati, N., Masulli, M., Di Ilio, C., & Parker, M. W. (1998). A mixed disulfide bond in bacterial glutathione transferase: Functional and evolutionary implications. *Structure*, 6(6), 721–734.
- Salentin, S., Schreiber, S., Haupt, V. J., Adasme, M. F., & Schroeder, M. (2015). PLIP: fully automated protein–ligand interaction profiler. *Nucleic Acids Research*, 43(W1), W443–W447.
- Santos, P. M., Mignogna, G., Heipieper, H. J., & Zennaro, E. (2002). Occurrence and properties of glutathione S-transferases in phenol-degrading *Pseudomonas* strains. *Research in Microbiology*, 153(2), 89–98.
- Sharma, R., Yang, Y., Sharma, A., Awasthi, S., & Awasthi, Y. C. (2004). Antioxidant role of glutathione S-transferases: Protection against oxidant toxicity and regulation of stress-mediated apoptosis. *Antioxidants and Redox Signaling*, 6(2), 289–300.
- Sheehan, D., meade, G., foley, V. M., & Dowd, C. A. (2001). Structure, function and evolution of glutathione transferases: Implications for classification of non-mammalian members of an ancient enzyme superfamily. *Biochemical Journal*, 360(1), 1–16.

- Shehu, D. (2018). *Molecular cloning, expression and enzymatic characterization of cytosolic glutathione stransferase from Acidovorax sp. KKS102* (Doctoral dissertation, University of Malaya). Retrieved from <http://studentsrepo.um.edu.my/11711/>
- Shehu, D., Abdullahi, N., & Alias, Z. (2019). Cytosolic glutathione S-transferase in bacteria: A review. *Polish Journal of Environmental Studies*, 28(2), 515–528.
- Shehu, D., & Alias, Z. (2018). Functional role of Tyr12 in the catalytic activity of novel zeta-like glutathione S-transferase from *Acidovorax* sp. KKS102. *Protein Journal*, 37(3), 261–269.
- Sherratt, P. J., & Hayes, J. D. (2002). Glutathione S-transferases. In C. Ioannides (Ed.), *Enzyme Systems that Metabolise Drugs and Other Xenobiotics* (pp. 319–352). John Wiley & Sons, Ltd.
- Shishido, T. (1981). Glutathione S-transferase from *Escherichia coli*. *Agricultural and Biological Chemistry*, 45(12), 2951–2953.
- Shuvo, M. H., Gulfam, M., & Bhattacharya, D. (2021). DeepRefiner: High-accuracy protein structure refinement by deep network calibration. *Nucleic Acids Research*, 49(W1), W147–W152.
- Skopelitou, K., Dhavala, P., Papageorgiou, A. C., & Labrou, N. E. (2012). A glutathione transferase from *Agrobacterium tumefaciens* reveals a novel class of bacterial GST superfamily. *PLoS ONE*, 7(4), 1–10.
- Slobodin, B., Han, R., Calderone, V., Vrielink, J. A. F. O., Loayza-Puch, F., Elkon, R., & Agami, R. (2017). Transcription impacts the efficiency of mRNA translation via co-transcriptional N6-adenosine methylation. *Cell*, 169(2), 326–337.e12.
- Stekel, D. (2018). First report of antimicrobial resistance pre-dates penicillin. *Nature*, 562(7726), 192–192.
- Stourman, N. V., Branch, M. C., Schaab, M. R., Harp, J. M., Ladner, J. E., & Armstrong, R. N. (2011). Structure and function of YghU, a Nu-class glutathione transferase related to YfcG from *Escherichia coli*. *Biochemistry*, 50(7), 1274–1281.
- Sun, D. (2018). Pull in and push out: Mechanisms of horizontal gene transfer in bacteria. *Frontiers in Microbiology*, 9(SEP), 1–8.
- Thai, T., Salisbury, B. H., & Zito, P. M. (2021). *Ciprofloxacin*. StatPearls Publishing.
- Thiriard, A., Raze, D., & Loch, C. (2020). Development and standardization of a high-throughput *Bordetella pertussis* growth-inhibition assay. *Frontiers in Microbiology*, 11, 777.
- Tripathi, V., & Cytryn, E. (2017). Impact of anthropogenic activities on the dissemination of antibiotic resistance across ecological boundaries. *Essays in Biochemistry*, 61(1), 11–21.
- Tsukada, M., Schröder, M., Roos, T. C., Chandraratna, R. A. S., Reichert, U., Merk, H. F., Orfanos, C. E., & Zouboulis, C. C. (2000). 13-Cis retinoic acid exerts its specific activity on human sebocytes through selective intracellular isomerization to all-trans retinoic acid and binding to retinoid acid receptors. *Journal of Investigative Dermatology*, 115(2), 321–327.

- Turella, P., Pedersen, J. Z., Caccuri, A. M., De Maria, F., Mastroberardino, P., Lo Bello, M., Federici, G., & Ricci, G. (2003). Glutathione transferase superfamily behaves like storage proteins for dinitrosyl-diglutathionyl-iron complex in heterogeneous systems. *Journal of Biological Chemistry*, 278(43), 42294–42299.
- van Hoek, A. H. A. M., Mevius, D., Guerra, B., Mullany, P., Roberts, A. P., & Aarts, H. J. M. (2011). Acquired antibiotic resistance genes: An overview. *Frontiers in Microbiology*, 2(SEP), 1–17.
- van Hylckama Vlieg, J. E. T., Kingma, J., Kruizinga, W., & Janssen, D. B. (1999). Purification of a glutathione S-transferase and a glutathione conjugate-specific dehydrogenase involved in isoprene metabolism in *Rhodococcus* sp. strain AD45. *Journal of Bacteriology*, 181(7), 2094–2101.
- Van Hylckama Vlieg, J. E. T., Leemhuis, H., Lutje Spelberg, J. H., & Janssen, D. B. (2000). Characterization of the gene cluster involved in isoprene metabolism in *Rhodococcus* sp. strain AD45. *Journal of Bacteriology*, 182(7), 1956–1963.
- Vuilleumier, S., & Pagni, M. (2002). The elusive roles of bacterial glutathione S-transferases: New lessons from genomes. *Applied Microbiology and Biotechnology*, 58(2), 138–146.
- Vuilleumier, Stéphane. (1997). Bacterial glutathione S-transferases: What are they good for? *Journal of Bacteriology*, 179(5), 1431–1441.
- Wadington, M. C., Ladner, J. E., Stourman, N. V., Harp, J. M., & Armstrong, R. N. (2009). Analysis of the structure and function of YfcG from *Escherichia coli* reveals an efficient and unique disulfide bond reductase. *Biochemistry*, 48(28), 6559–6561.
- Wang, X.-Y., Zhang, Z.-R., & Perrett, S. (2009). Characterization of the activity and folding of the glutathione transferase from *Escherichia coli* and the roles of residues Cys10 and His106. *Biochemical Journal*, 417(1), 55–64.
- Wikteliu, E., & Stenberg, G. (2007). Novel class of glutathione transferases from cyanobacteria exhibit high catalytic activities towards naturally occurring isothiocyanates. *Biochemical Journal*, 406(1), 115–123.
- Williams, C. J., Headd, J. J., Moriarty, N. W., Prisant, M. G., Videau, L. L., Deis, L. N., Verma, V., Keedy, D. A., Hintze, B. J., Chen, V. B., Jain, S., Lewis, S. M., Arendall, W. B., Snoeyink, J., Adams, P. D., Lovell, S. C., Richardson, J. S., & Richardson, D. C. (2018). MolProbity: More and better reference data for improved all-atom structure validation. *Protein Science*, 27(1), 293–315.
- Xiang, Z. (2006). Advances in homology protein structure modeling. *Current Protein & Peptide Science*, 7(3), 217–227.
- Zablotowicz, R. M., Hoagland, R. E., Locke, M. A., & Hickey, W. J. (1995). Glutathione-S-transferase activity and metabolism of glutathione conjugates by rhizosphere bacteria. *Applied and Environmental Microbiology*, 61(3), 1054–1060.
- Zhou, N. Y., Fuenmayor, S. L., & Williams, P. A. (2001). nag genes of *Ralstonia* (formerly *Pseudomonas*) sp. strain U2 encoding enzymes for gentisate catabolism. *Journal of Bacteriology*, 183(2), 700–708.